Stony Brook University

Center for Frontiers in Nuclear Science

Groomed Event Shapes in e+p DIS + Lessons for EIC*

Henry Klest for the H1 Collaboration

HERA4EIC Workshop, June 8

*EIC Lessons are my personal opinions as a newcomer, not representative of the H1 collaboration!

FAR BEYOND

Event Shapes

$$\tau = 1 - T \quad \text{with} \quad T = \frac{\sum_h |\vec{p}_{z,h}|}{\sum_h |\vec{p}_h|}$$

- Inclusive observables where all particles contribute
  - E.g. Thrust – measures degree of collimation along an axis
- **Sensitive to QCD across scales**
- Calculable to high precision in perturbation theory
  - Fixed-order QCD → tail of thrust distribution
  - Soft-collinear effective theory (SCET) calculations → peak of thrust distribution
- Used extensively in e^+e^- and Breit frame e+p collisions

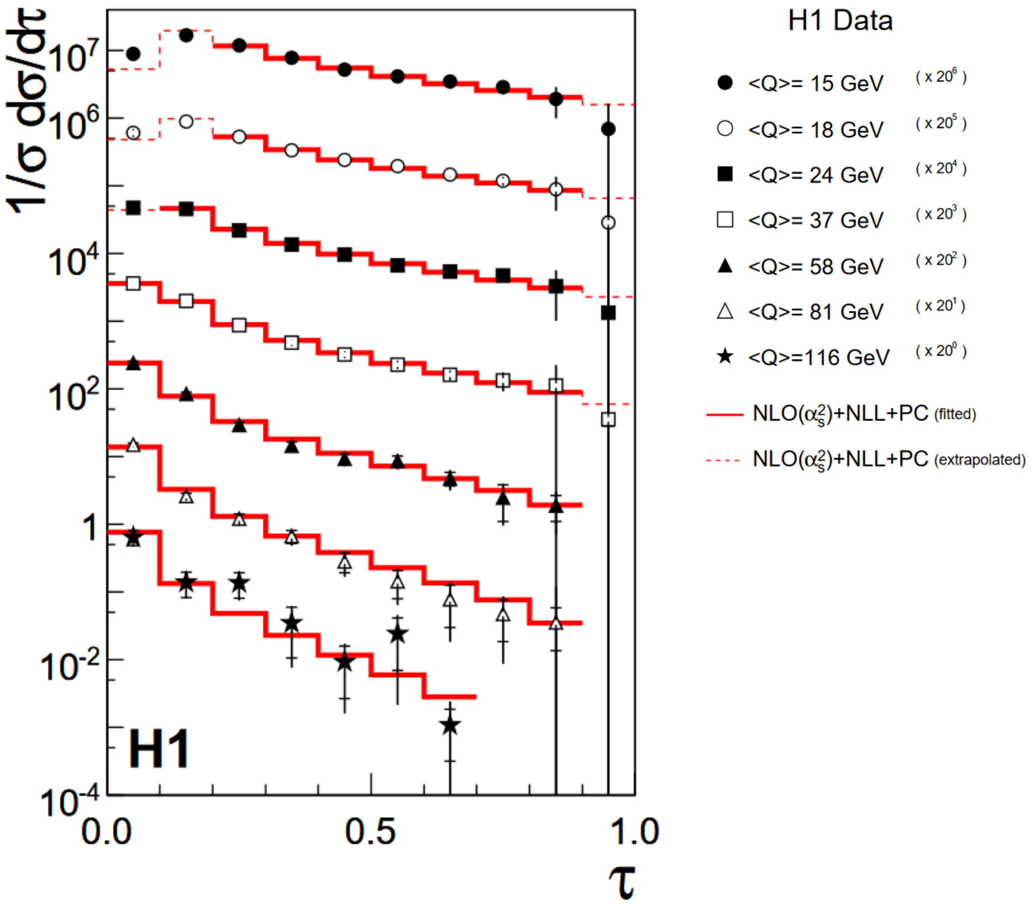

arXiv/0512014v1

Inclusive DIS & Breit Frame

- HERA-II data
  - $Q^2 > 150$ GeV^2, $0.2 < y < 0.7$
  - No direct $x_{Bj.}$ cut applied
  - 352 pb^{-1} collected

- Breit Frame
  - Defined as the frame where $2x_{Bj.}P + q = 0$
  - Exchanged boson reverses struck parton's momentum
    - Parton has $\overrightarrow{xP}$ incoming, $-\overrightarrow{xP}$ outgoing

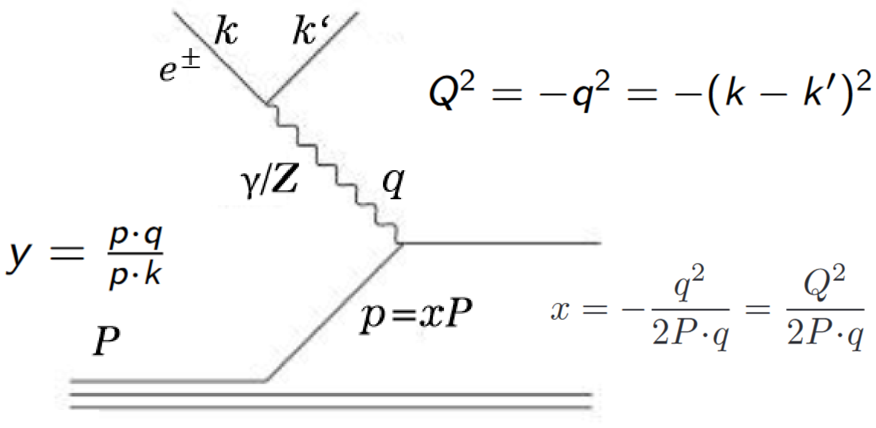

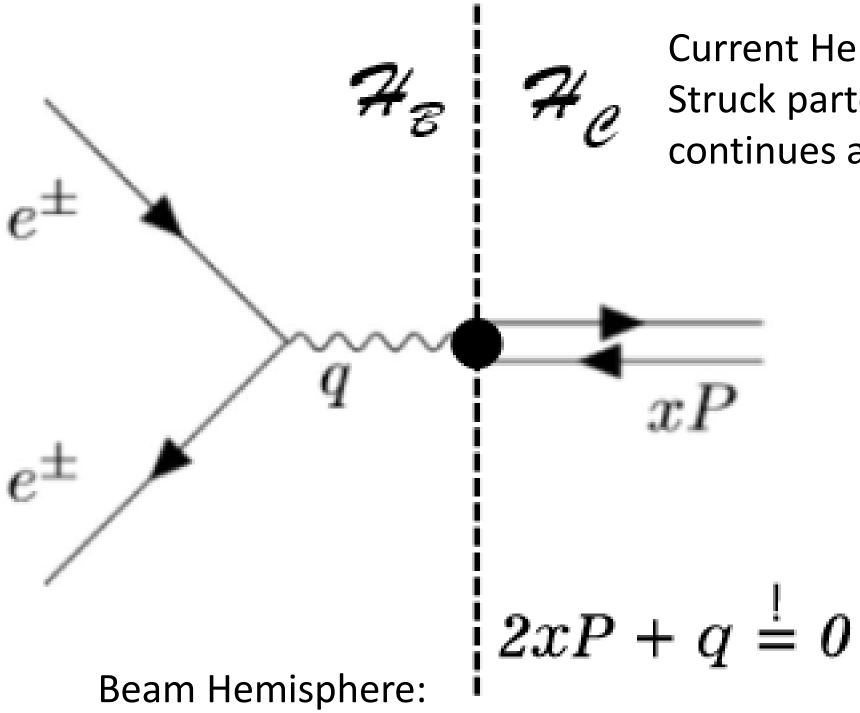

Current Hemisphere: Struck parton continues at η = -∞

Beam Hemisphere: Proton remnant continues at η = ∞

Inclusive DIS – Event Selection

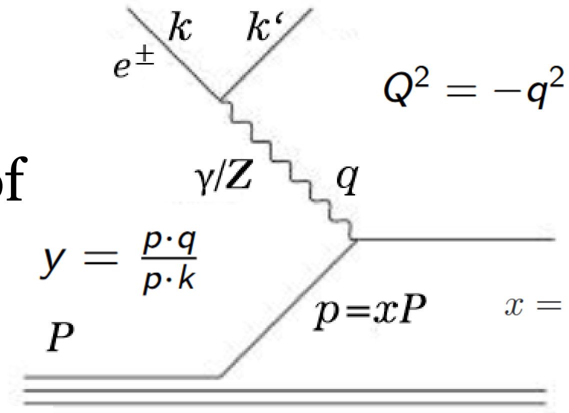

$$Q^2 = -q^2 = -(k-k')^2$$

$$x = -\frac{q^2}{2P\cdot q} = \frac{Q^2}{2P\cdot q}$$

- DIS kinematics reconstructed with IΣ method
  - Factors out QED ISR
  - Does **not** assume that incoming electron has 27.6 GeV of energy at the hard vertex
    - Infer electron energy from longitudinal momentum balance
- Require 50 GeV < $\Sigma(E-P_z)$ < 60 GeV
  - Ensures low amount of QED ISR and detector losses in current hemisphere
    - Effectively constrains an unmeasured ISR photon to have < 2.5 GeV of energy
    - Also removes all non-DIS background (photoproduction, beam-gas, etc.)
- Fiducial volume cut applied to ensure high electron purity

$$E_{I\Sigma}^{e'} = \frac{\Sigma_{HFS} + E_{e'}(1-\cos\theta_{e'})}{2}$$

$$x_{I\Sigma} = \frac{E_{e'}}{E_p}\frac{\cos^2\theta/2}{y_\Sigma}$$

$$y_{I\Sigma} = y_\Sigma = \frac{\Sigma}{\Sigma + E(1-\cos\theta)}$$

$$Q^2_{I\Sigma} = \frac{E^2\sin^2\theta}{1-y_\Sigma}$$

arXiv:2006.10751

Centauro

- Jet algorithm with asymmetric clustering distance measure
  - Suited for clustering Born-level DIS in the Breit frame

- Here Centauro is used to produce a clustering tree for the full event

Definition:

$$d_{ij} = (\bar{\eta}_i - \bar{\eta}_j)^2 + 2\bar{\eta}_i\bar{\eta}_j(1 - \cos(\phi_i - \phi_j))$$

Breit frame

$$\bar{\eta}_i = 2\sqrt{1 + \frac{q \cdot p_i}{x_B P \cdot p_i}} \xrightarrow[\text{frame}]{\text{Breit}} \frac{2p_i^{\perp}}{p_i^{+}}$$

Limits:

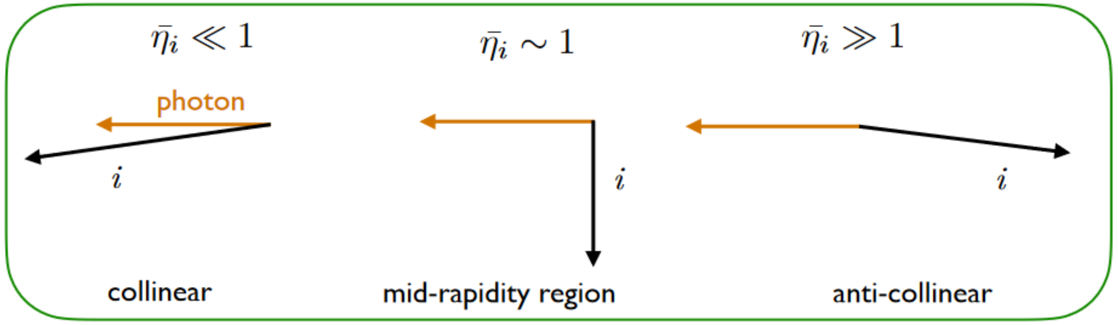

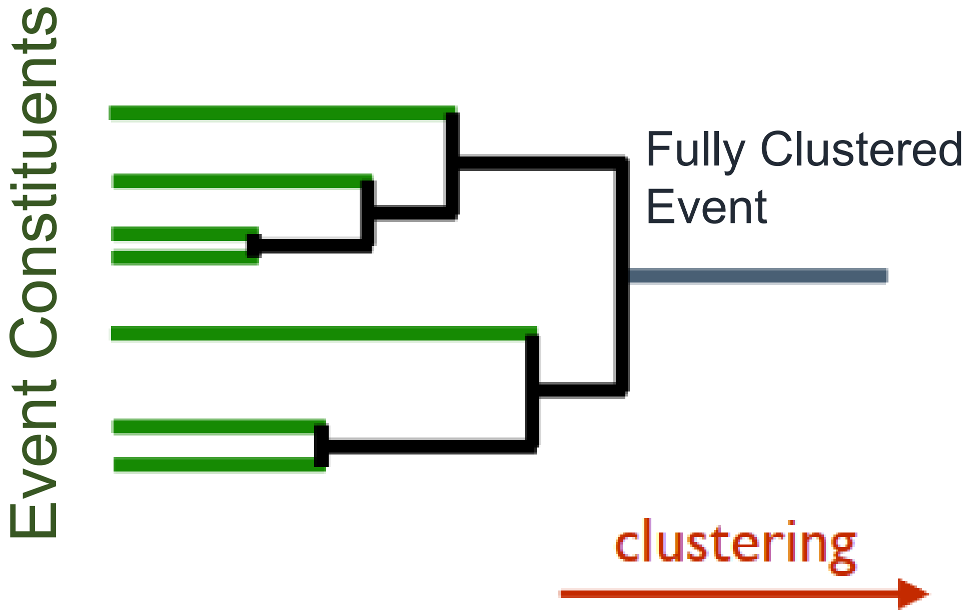

Figures courtesy of Y. Makris [2]

Centauro jets will be an important EIC measurement!

Centauro

$$d_{ij} = \min(p_{Ti}^{2p}, p_{Tj}^{2p})\Delta R_{ij}^2/R^2 \, , \qquad d_{iB} = p_{Ti}^{2p}$$

vs.

$$d_{ij} = (\Delta\bar{\eta}_{ij})^2 + 2\bar{\eta}_i\bar{\eta}_j(1 - \cos\Delta\phi_{ij}) \, ,$$

where

$$\bar{\eta}_i \equiv 2\sqrt{1 + \frac{q \cdot p_i}{x_B P \cdot p_i}} \xrightarrow[\text{frame}]{\text{Breit}} \frac{2p_i^{\perp}}{p_i^{+}} \, ,$$

vs.

$$d_{ij} = \min(E_i^{2p}, E_j^{2p})\frac{1 - c_{ij}}{1 - c_R} \, , \qquad d_{iB} = E_i^{2p}$$

where $c_{ij} = \cos\theta_{ij}$ and $c_R = \cos R$.

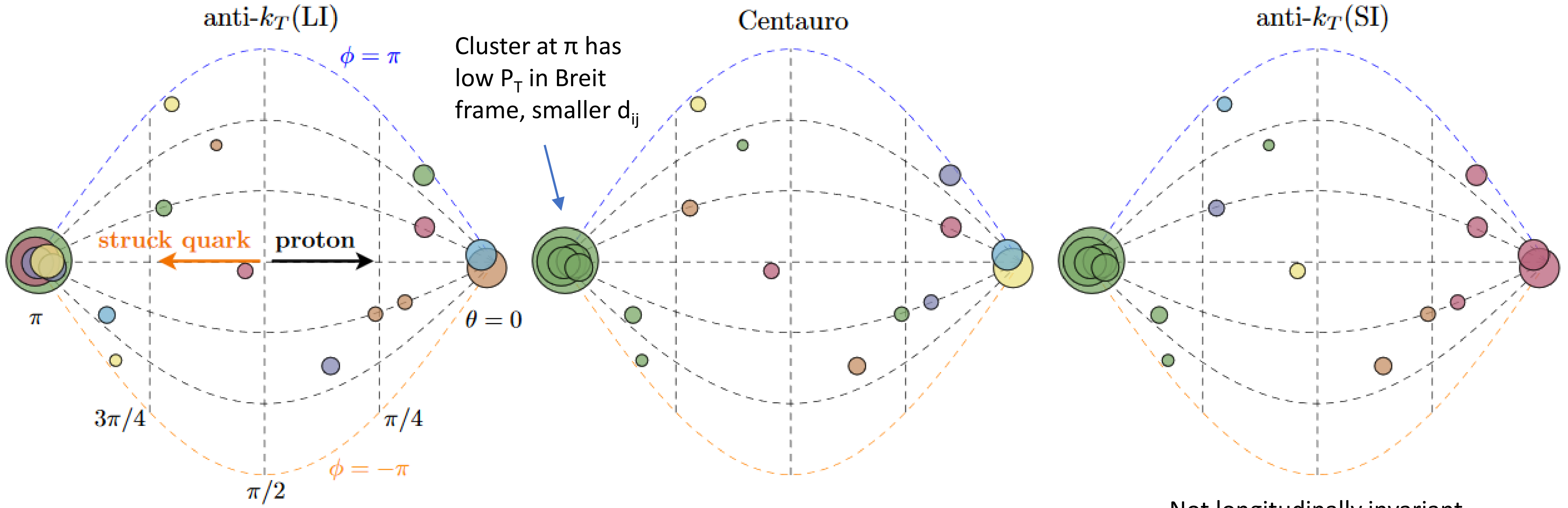

Doesn't preferentially capture struck quark

Not longitudinally invariant

Figure 2. Jet clustering in the Breit frame using the longitudinally-invariant anti-k_T(LI), Centauro, and spherically-invariant anti-k_T(SI) algorithms in a DIS event simulated with PYTHIA 8. Each particle is illustrated as a disk with area proportional to its energy and the position corresponds to the direction of its momentum projected onto the unfolded sphere about the hard-scattering vertex. The vertical dashed lines correspond to constant θ and curved lines to constant ϕ. All the particles clustered into a given jet are colored the same.

Event Grooming in DIS

- Whole event is clustered into one “jet”

- Iteratively de-cluster until grooming condition is passed
  - Analogous to Soft Drop in p+p

- Groomed events are similar to groomed jets!

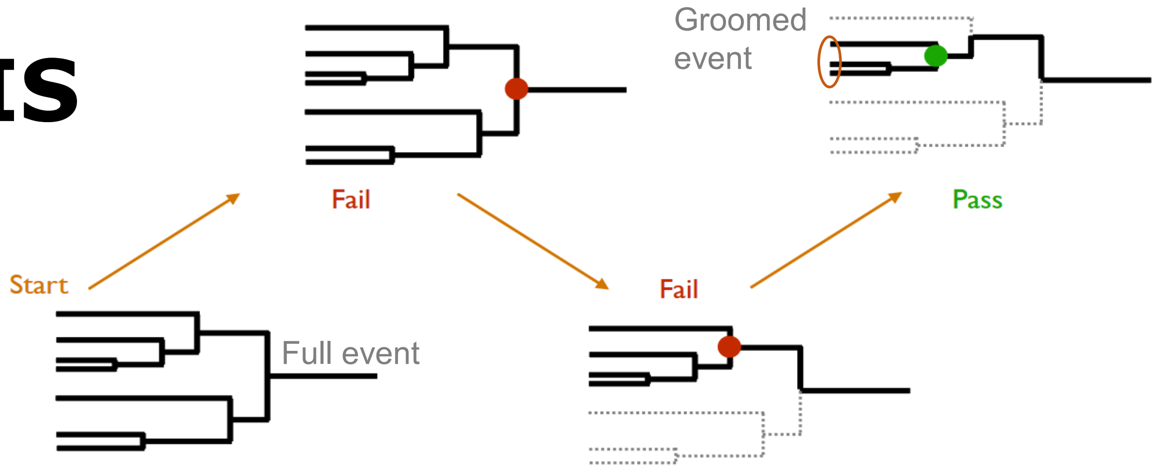

$$z_i = \frac{P \cdot p_i}{P \cdot q} \xrightarrow[\text{frame}]{\text{Breit}} z_i = n \cdot p_i / Q = p_i^+ / Q\,.$$

Limits (geometric interpretation in the Breit frame)

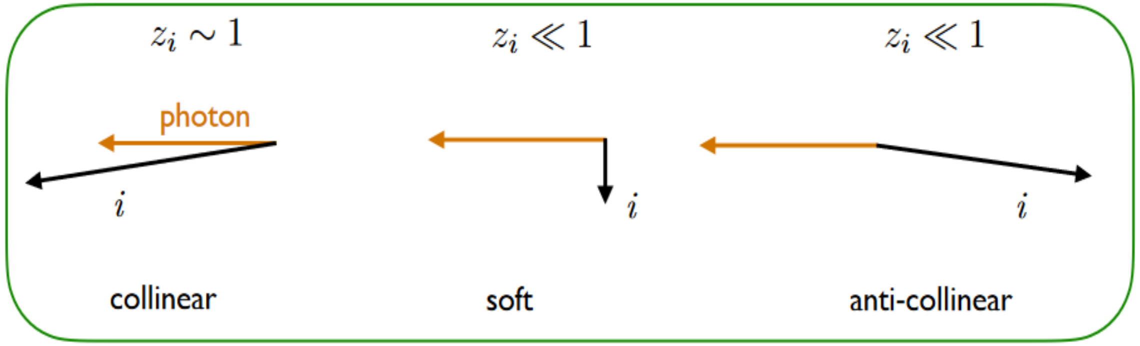

$$\frac{\min(p_{t1}, p_{t2})}{p_{t1} + p_{t2}} > z_{\text{cut}} \longrightarrow \frac{\min(z_i, z_j)}{z_i + z_j} > z_{\text{cut}}$$

p+p Soft Drop condition

DIS grooming condition

Breit Frame Event Displays

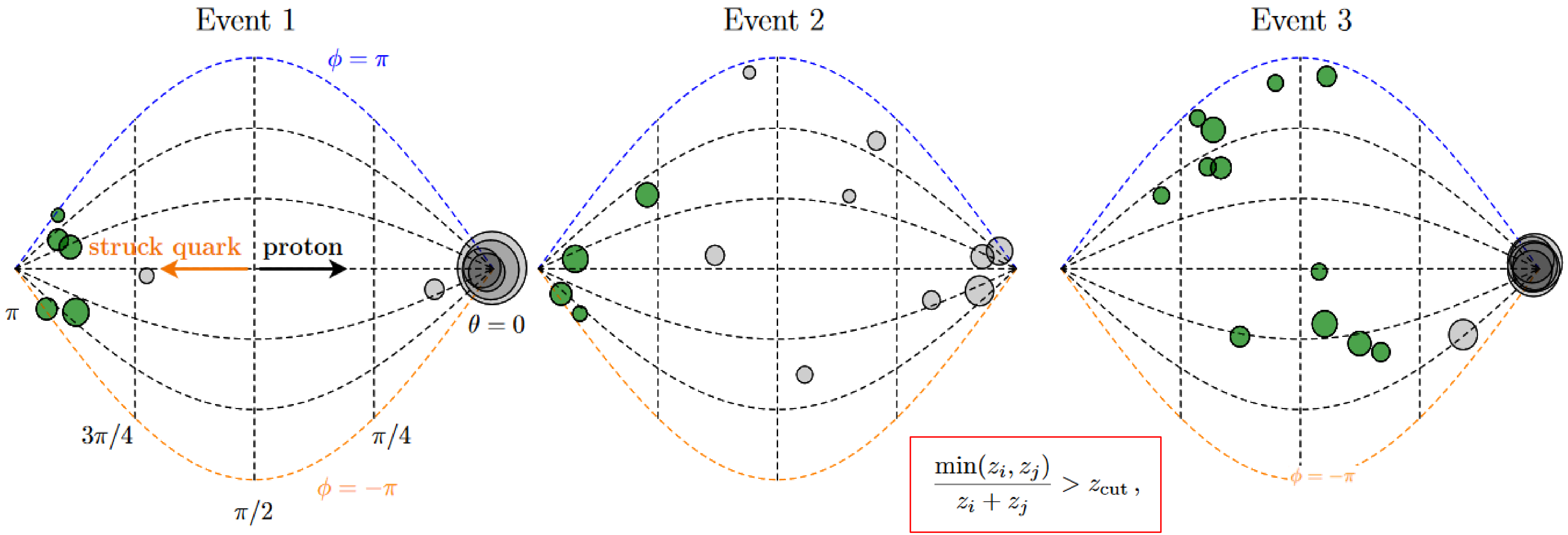

$$\frac{\min(z_i, z_j)}{z_i + z_j} > z_{\mathrm{cut}} \,,$$

Figure 2. Visualization of three PYTHIA 8 events at $\sqrt{s} = 63$ GeV and $Q \sim 10$ GeV before and after grooming. The particles in this events are represented by disks on the unfolded sphere. Green disks represent particles that pass grooming where grayed-out particles are removed from the event by the grooming procedure. For the grooming parameter we use here $z_{\mathrm{cut}} = 0.1$

Grooming Benefits

- No underlying event, why groom?
  - Less affected by lab-frame detector acceptance
  - Mitigate QCD remnant, ISR
  - No theoretically challenging non-global logarithms
- Ungroomed detector-level shows significant difference from particle-level
  - Detector acceptance, efficiencies
- Grooming events brings particle-level and detector-level distributions into much better agreement!

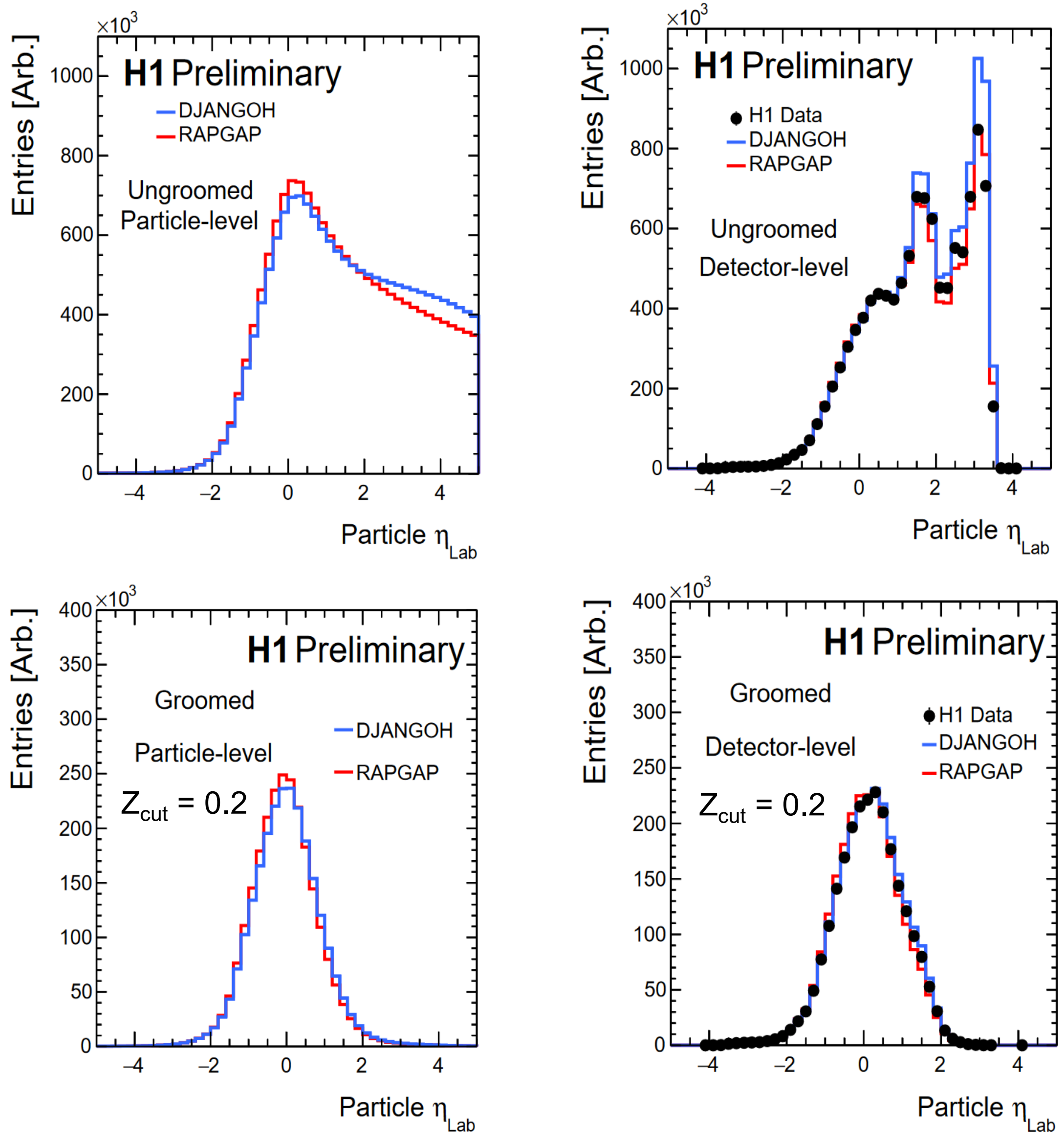

Observables

- After grooming procedure, a subset of particles survives
  - Event shape is calculated with these particles
  - Two event shapes studied here

- Groomed Invariant Mass (GIM) $M^2_{Gr.} = (\sum_i p_i^\mu)^2$

- Groomed 1-Jettiness τ_1^b (analogous to thrust)

$$\tau_1 = \frac{2}{Q^2} \sum_{i \in \text{gr. ent.}} \min(q_B \cdot p_i,\, q_J \cdot p_i)$$

$$\tau_1^b \rightarrow \quad q_J = q + xP, \quad q_B = xP$$

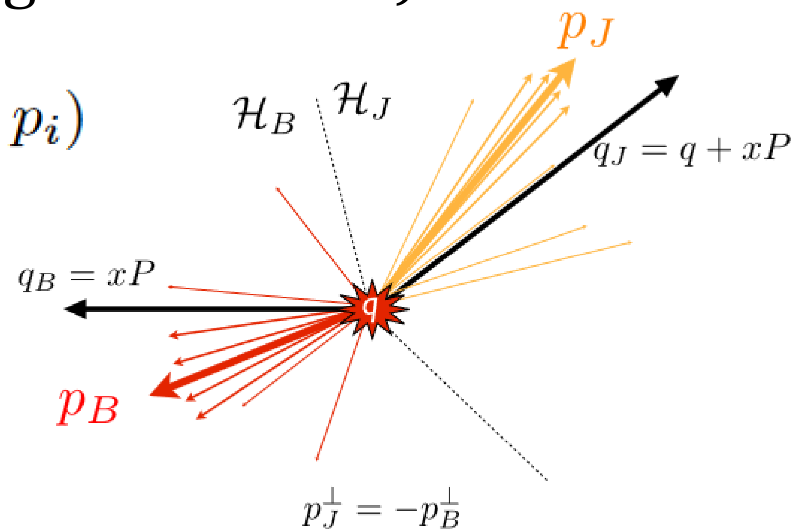

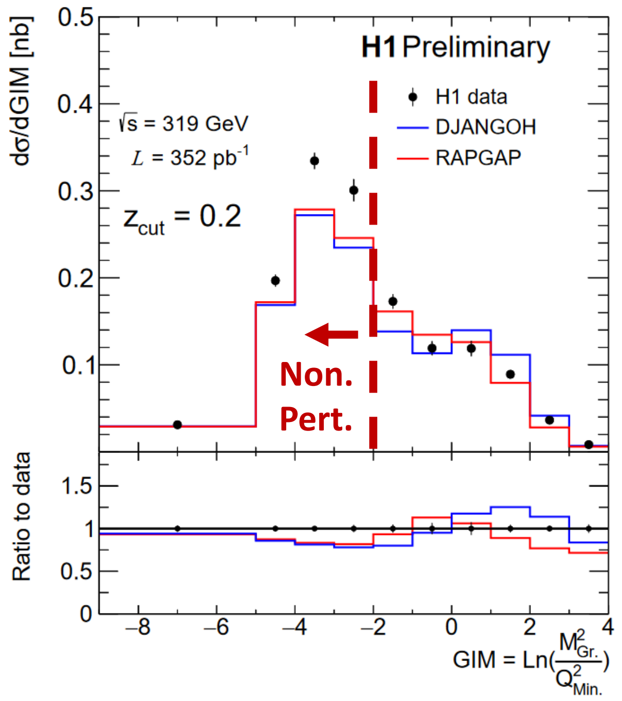

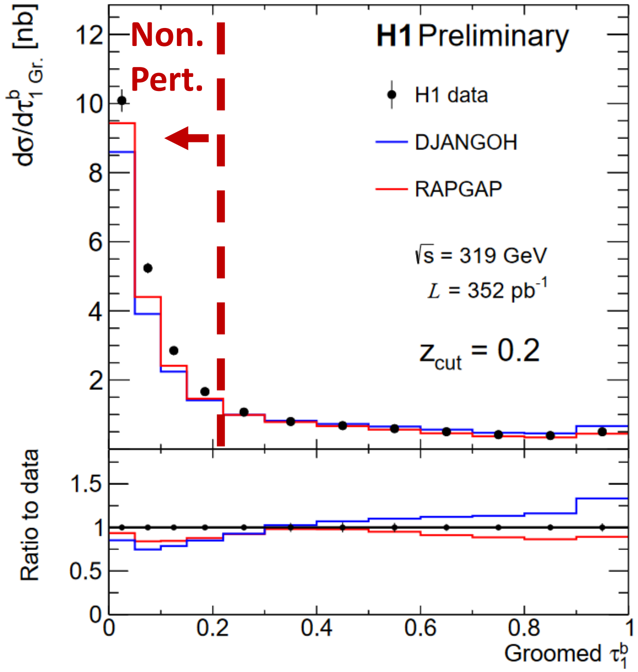

Observables

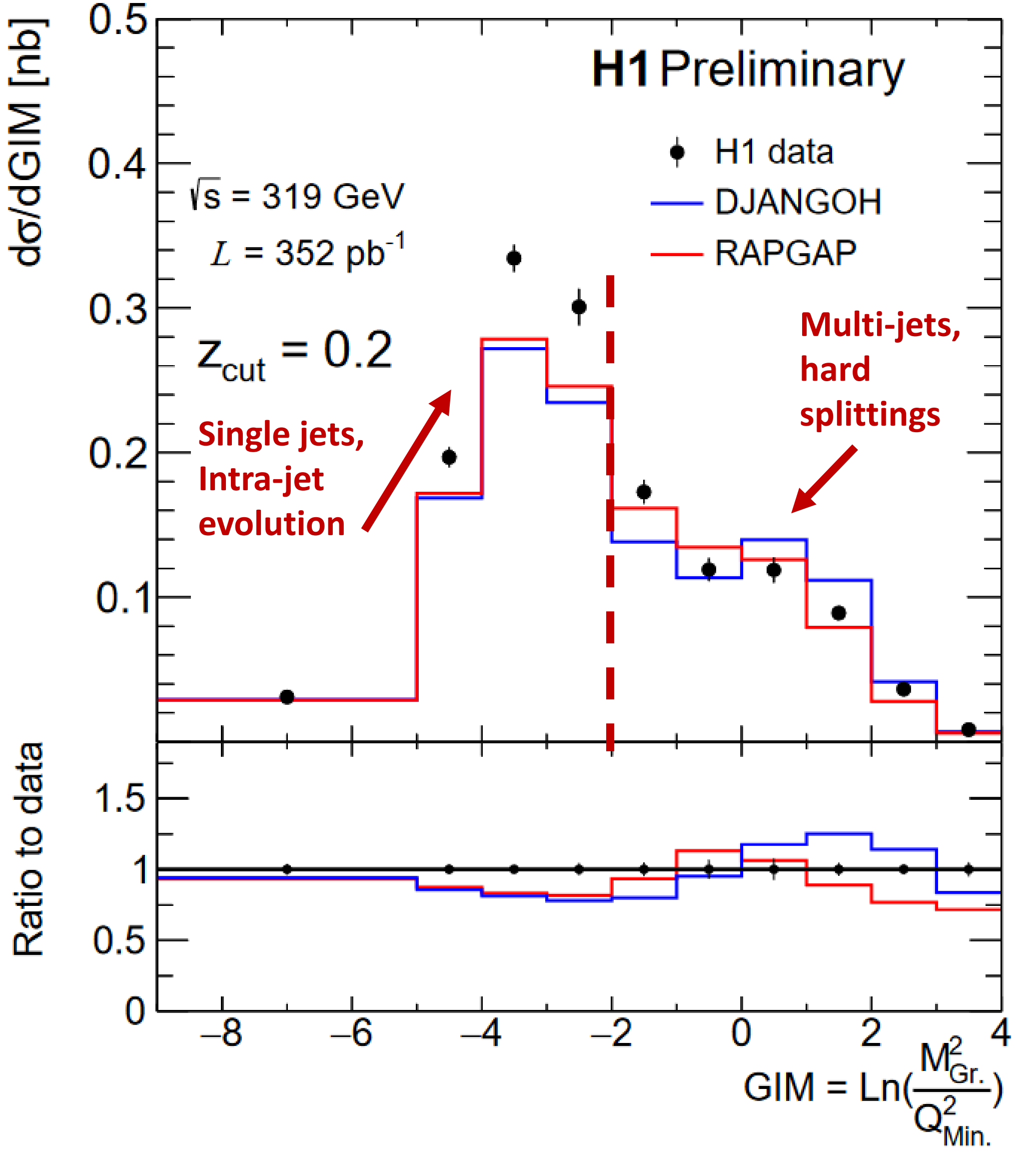

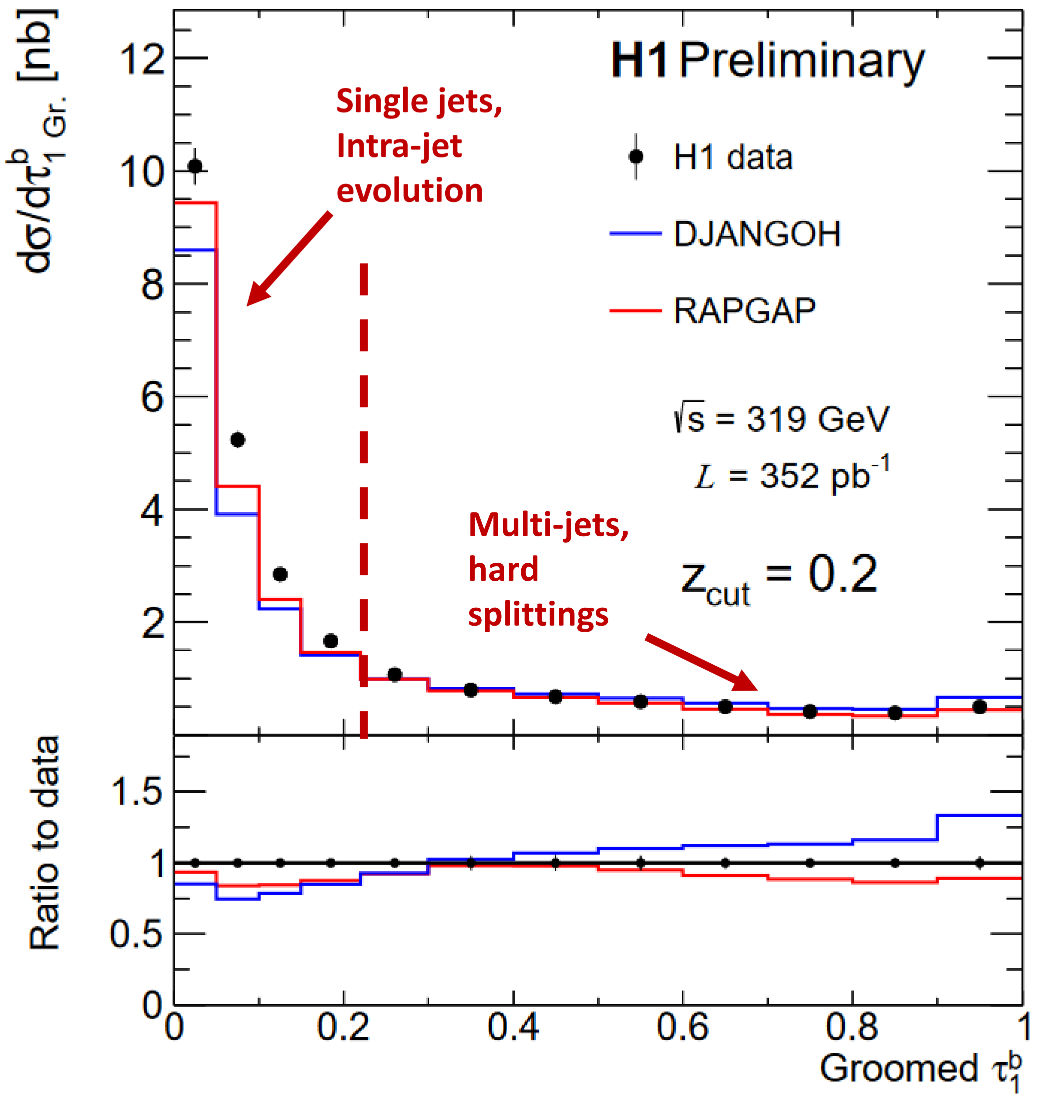

Groomed vs. Ungroomed 1-jettiness

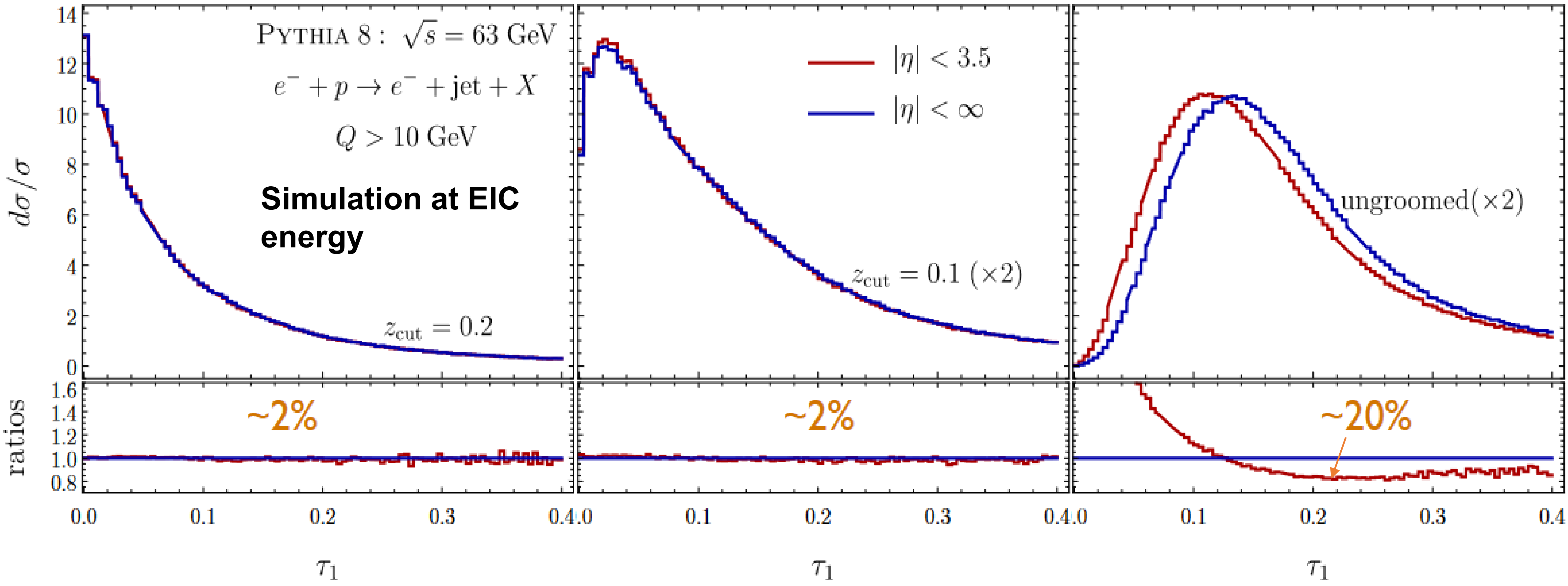

Grooming enables precision measurement!

Groomed Invariant Mass - Factorization

$$\lambda = \frac{m^2_{\text{gr.}}}{Q^2} \,,$$

$$p = (p^+, p^-, p^\perp)$$

$$n\text{-collinear:} \quad p_n \sim Q(z_{\text{cut}}, 1, \sqrt{z_{\text{cut}}}) \,,$$

$$\text{soft:} \quad p_s \sim Q z_{\text{cut}}(1,1,1) \,,$$

$$\text{collinear-soft:} \quad p_{cs} \sim Q(\lambda, z_{\text{cut}}, \sqrt{z_{\text{cut}}\lambda}) \,,$$

$$\bar{n}\text{-collinear:} \quad p_{\bar{n}} \sim Q(1, \lambda, \sqrt{\lambda}) \,,$$

region 1: $1 \gg z_{\text{cut}} \gg m^2_{\text{gr.}}/Q^2$

Jet Direction (Breit η=-∞) = $\bar{n}$-collinear direction

Beam Direction (Breit η=-∞) = n-collinear direction

Soft Radiation (Isotropic)

Collinear-soft radiation, wide-angle soft radiation mostly along jet direction

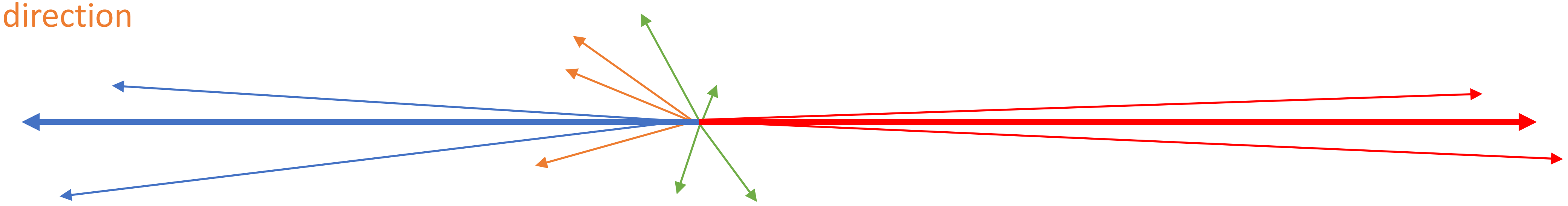

$$\frac{d\sigma}{dx dQ^2 dm^2_{\text{gr.}}} = H(Q, y, \mu) S(Q z_{\text{cut}}, \mu) \sum_f \mathcal{B}_{f/P}(x, Q^2 z_{\text{cut}}, \mu) \int de_{\bar{n}} de_{cs}\, \delta(m^2_{\text{gr.}} - e_{\bar{n}} - e_{cs}) J(e_{\bar{n}}, \mu^2) \mathcal{C}(e_{cs} z_{\text{cut}}, \mu^2)$$
$$\times \left[1 + \mathcal{O}\left(z_{\text{cut}}, \frac{m^2_{\text{gr.}}}{z_{\text{cut}} Q^2}\right)\right] , \quad (15)$$

In Region 1, shape of distribution should depend only on jet and collinear-soft functions, which are independent of Q

Groomed Invariant Mass - Factorization

$$\lambda = \frac{m_{\text{gr.}}^2}{Q^2} \,,$$

$$p = (p^+, p^-, p^\perp)$$

n-collinear: $p_n \sim Q(z_{\text{cut}}, 1, \sqrt{z_{\text{cut}}})$,

soft: $p_s \sim Q z_{\text{cut}}(1,1,1)$,

collinear-soft: $p_{cs} \sim Q(\lambda, z_{\text{cut}}, \sqrt{z_{\text{cut}}\lambda})$,

$\bar{n}$-collinear: $p_{\bar{n}} \sim Q(1, \lambda, \sqrt{\lambda})$,

region 1: $1 \gg z_{\text{cut}} \gg m_{\text{gr.}}^2/Q^2$

Grooming causes only Jet and Collinear-soft radiation to contribute to shape of distribution in the single-jet (low invariant mass) limit!

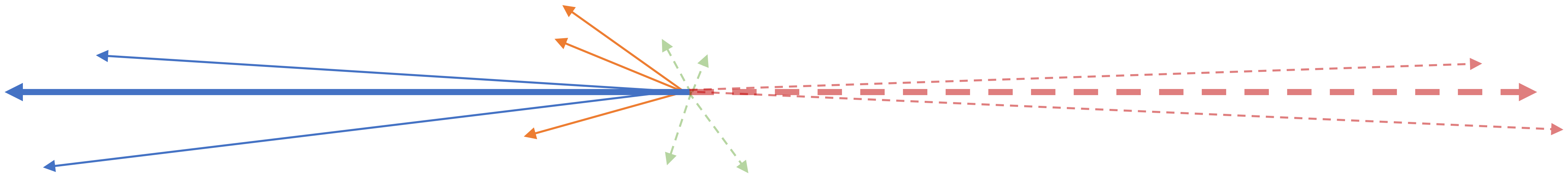

$$\frac{d\sigma}{dx\,dQ^2\,dm_{\text{gr.}}^2} = H(Q,y,\mu) S(Q z_{\text{cut}}, \mu) \sum_f \mathcal{B}_{f/P}(x, Q^2 z_{\text{cut}}, \mu) \int de_{\bar{n}}\, de_{cs}\, \delta(m_{\text{gr.}}^2 - e_{\bar{n}} - e_{cs}) J(e_{\bar{n}}, \mu^2)\, \mathcal{C}(e_{cs} z_{\text{cut}}, \mu^2)$$
$$\times \left[1 + \mathcal{O}\left(z_{\text{cut}}, \frac{m_{\text{gr.}}^2}{z_{\text{cut}} Q^2}\right)\right] , \quad (15)$$

In Region 1, shape of distribution should depend only on jet and collinear-soft functions, which are independent of Q

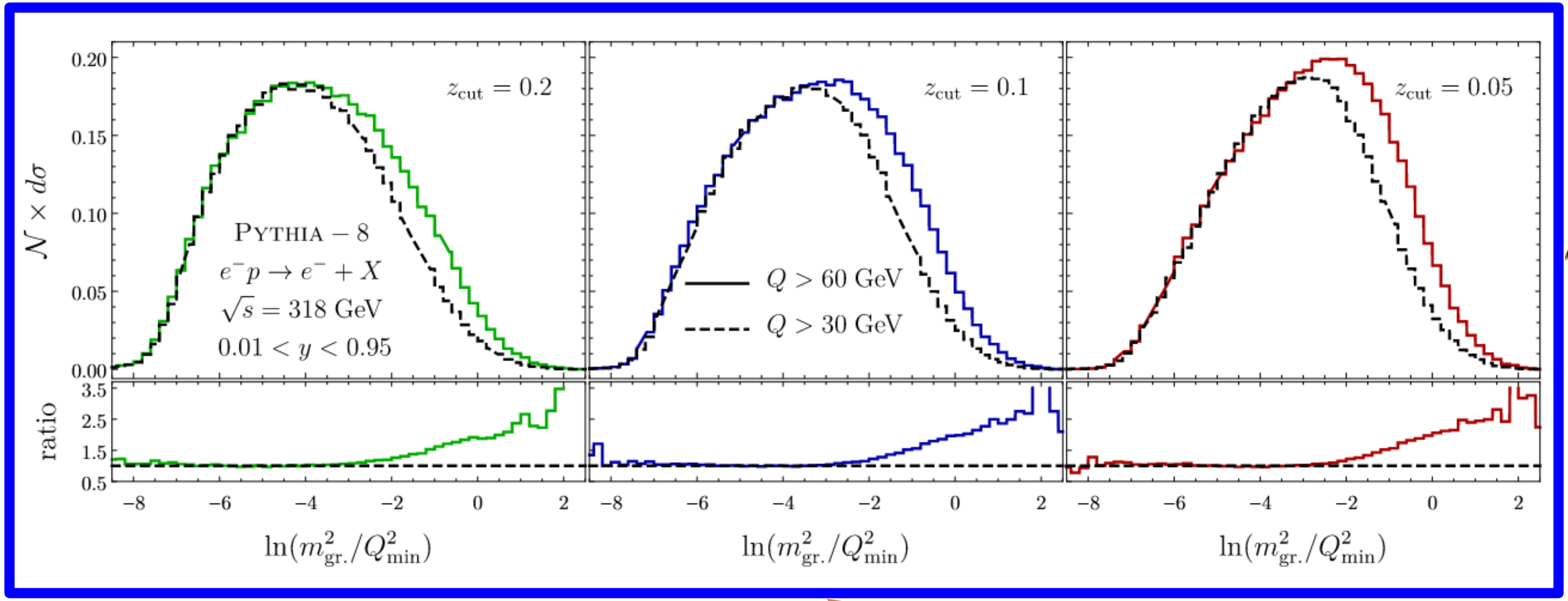

$= (p^+, p^-, p^\perp)$

$\sim Q(z_{\rm cut}, 1, \sqrt{z_{\rm cut}})$,

$\sim Q z_{\rm cut}(1, 1, 1)$,

$\sim Q(\lambda, z_{\rm cut}, \sqrt{z_{\rm cut}\lambda})$,

$\sim Q(1, \lambda, \sqrt{\lambda})$,

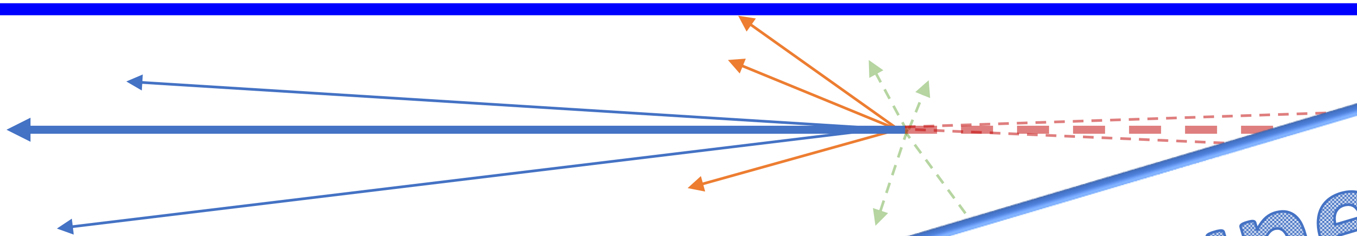

Stay tuned for an test of this prediction!

$$\frac{d\sigma}{dx dQ^2 dm^2_{\rm gr.}} = H(Q, y, \mu) S(Q z_{\rm cut}, \mu) \sum_f \mathcal{B}_{f/P} \cdots (\ldots_{cs} z_{\rm cut}, \mu^2)$$

$$\times \left[1 + \mathcal{O}\left(z_{\rm cut}, \frac{m^2_{\rm gr.}}{z_{\rm cut} Q^2}\right)\right], \quad (15)$$

Shape of distribution should depend only on jet and collinear-soft functions, which are independent of Q!

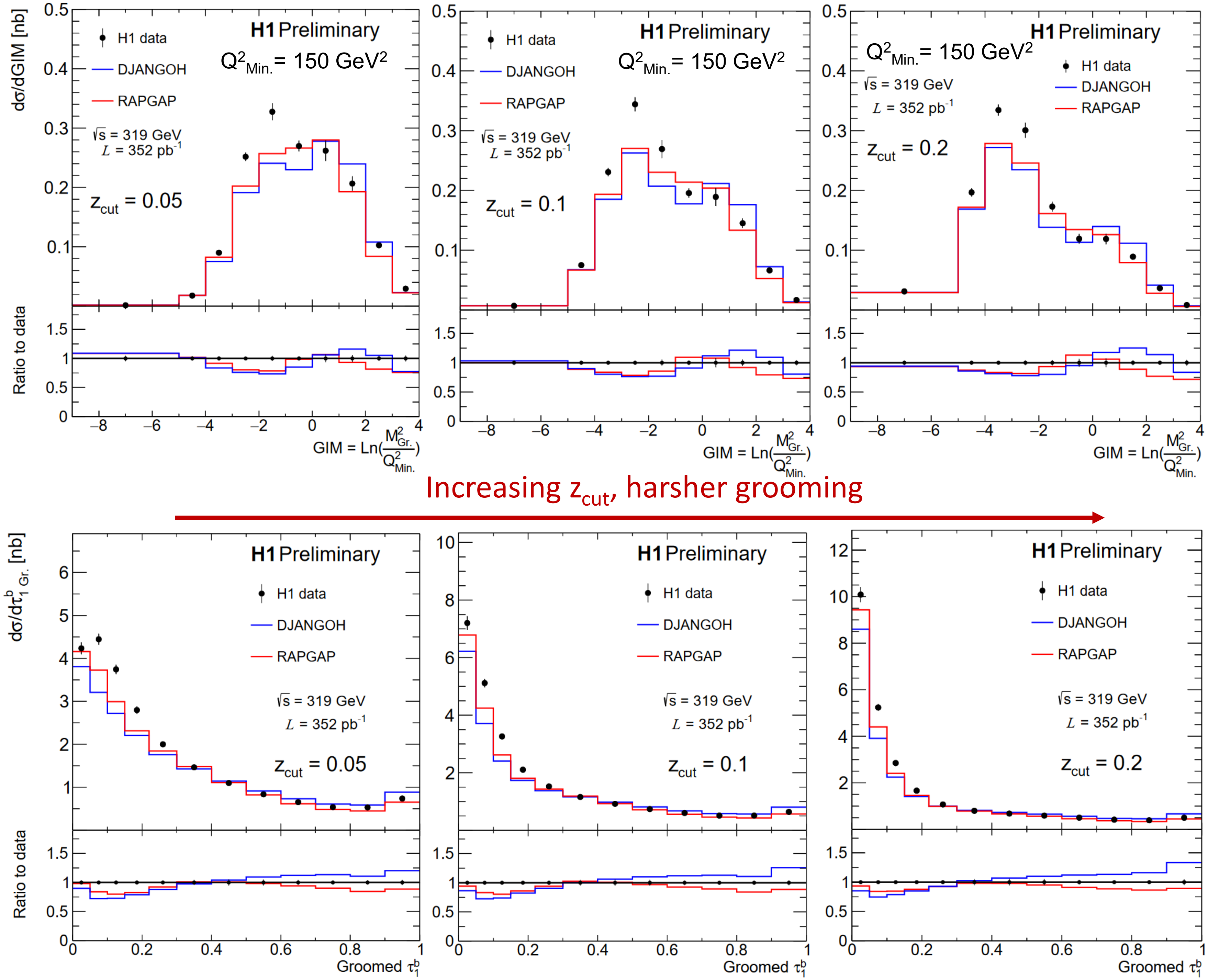

Results

- Data is corrected for real QED ISR and FSR
- Uncertainty on data is statistical ⊕ systematic
  - Dominated by model uncertainty from bin-by-bin correction
- RAPGAP and DJANGOH
  - Standard H1 MCs
  - Both use LEPTO for matrix elements $O(\alpha_S)$
- DJANGOH:
  - Color dipole model PS + string fragmentation
- RAPGAP:
  - DGLAP PS + string fragmentation

Results – Groomed 1 Jettiness

$$\tau_1 = \frac{2}{Q^2}\sum_{i\in \mathrm{gr.\ ent.}} \min(q_B\cdot p_i,\, q_J\cdot p_i)$$

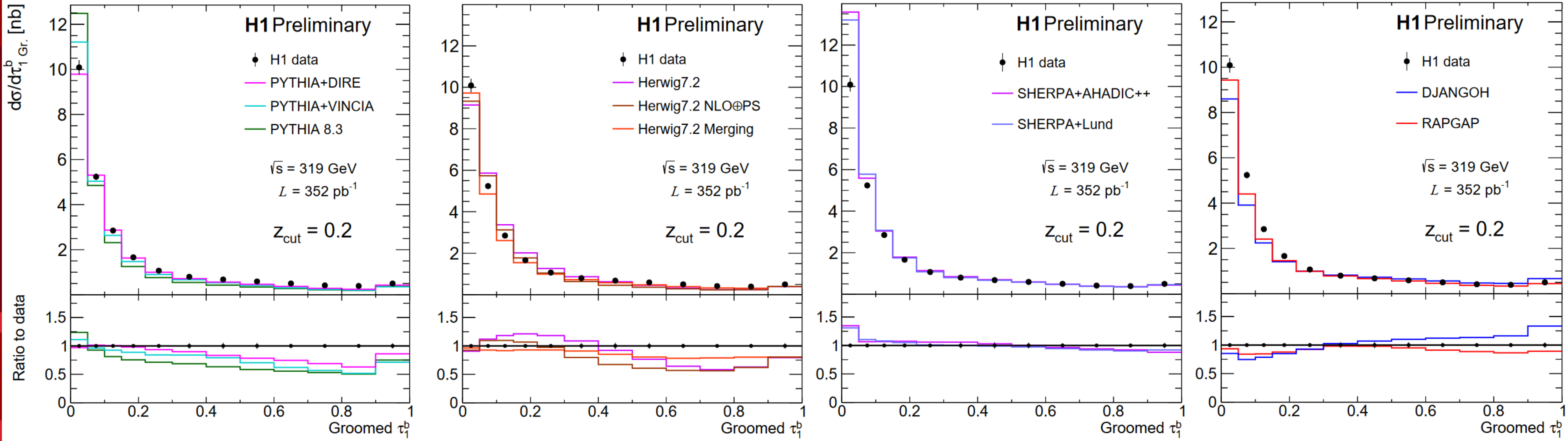

- PYTHIA – Version 8.3
  - VINCIA – Antenna Shower
  - DIRE - Dipole shower + multijet merging
- Herwig – Version 7.2 (Angular-ordered)
  - NLO ⊕PS – AO Shower, subtractive matching
  - Merging - Dipole shower + multijet merging
- SHERPA – Version 2.2.12 (MEPS@NLO)
  - AHADIC++ - Cluster Fragmentation
  - Lund – String Fragmentation

- Best tail region from SHERPA, RAPGAP
  - Fixed-order, multijets, hard splittings
- Best peak region from DIRE, Herwig Merging
  - Resummation, parton shower, hadronization

Results – Groomed Invariant Mass

$$M^2_{Gr.} = (\sum_i p_i^{\mu})^2$$

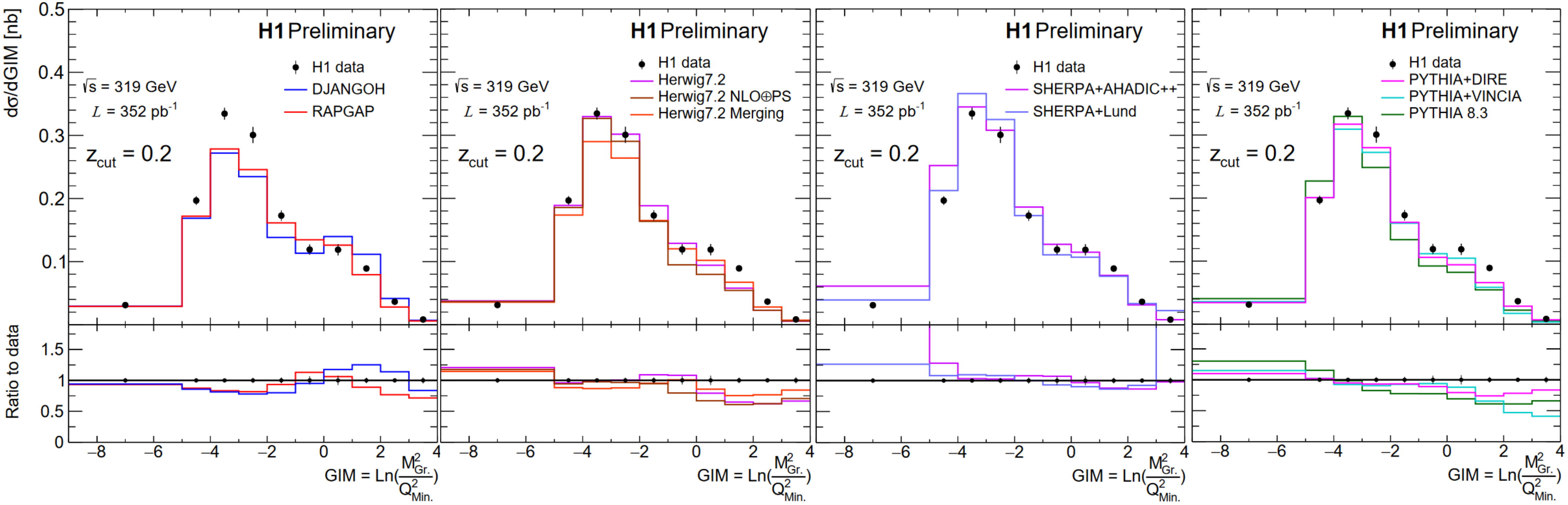

- PYTHIA – Version 8.3
  - VINCIA – Antenna Shower
  - DIRE - Dipole shower + multijet merging
- Herwig – Version 7.2 (Angular-ordered)
  - NLO ⊕PS – AO Shower, subtractive matching
  - Merging - Dipole shower + multijet merging
- SHERPA – Version 2.2.12 (MEPS@NLO)
  - AHADIC++ - Cluster Fragmentation
  - Lund – String Fragmentation

- $Q^2_{Min.}$ = 150 GeV²
- Best high mass region from SHERPA
  - Fixed-order, multijets, hard splittings
- Best low mass region from Herwig, DIRE
  - Resummation, parton shower, hadronization

Results – Groomed Invariant Mass

$M^2_{Gr.} = (\sum_i p_i^\mu)^2$

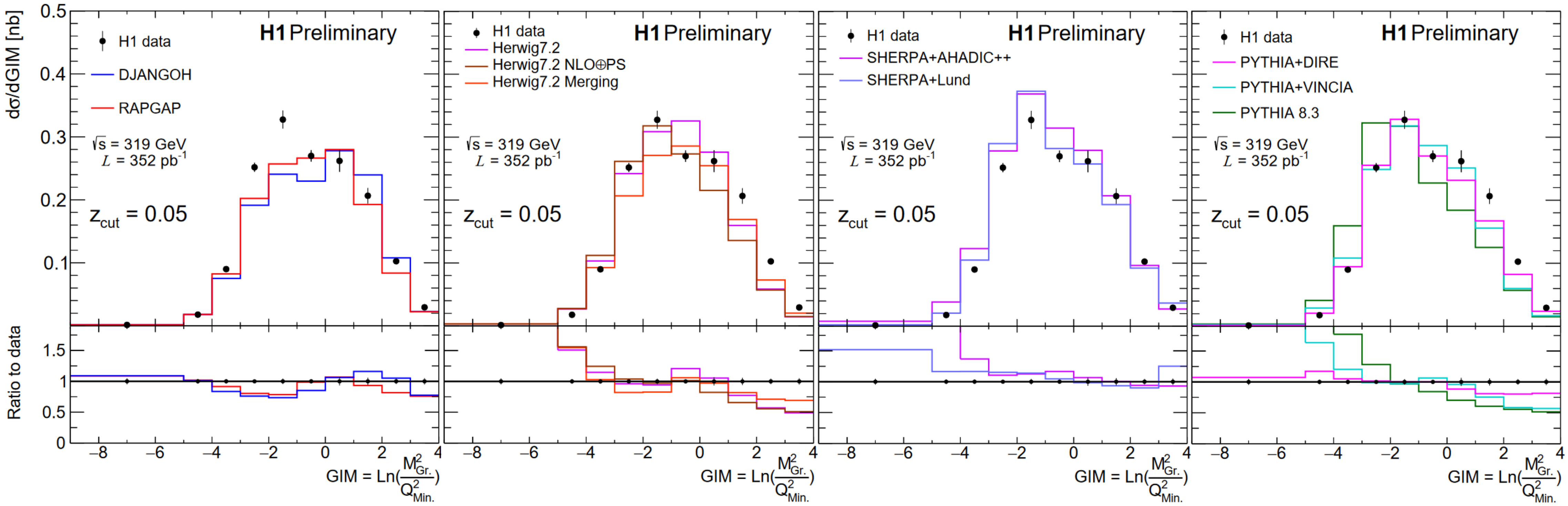

- PYTHIA – Version 8.3
  - VINCIA – Antenna Shower
  - DIRE - Dipole shower + multijet merging
- Herwig – Version 7.2 (Angular-ordered)
  - NLO ⊕PS – AO Shower, subtractive matching
  - Merging - Dipole shower + multijet merging
- SHERPA – Version 2.2.12 (MEPS@NLO)
  - AHADIC++ - Cluster Fragmentation
  - Lund – String Fragmentation

- Generally, predictions become less accurate at lower z_{cut}
  - Less grooming → Less removal of remnant hemisphere radiation
  - Remnant hemisphere is typically less well described by MC models

Comparison to Analytic Prediction

- Analytic - SCET
  - From Y. Makris [1]
  - Evaluated at two values of Ω_{NP}
    - Shape function mean
  - No fixed-order calculation yet incorporated
- Agreement improves with increasing z_{cut}, Ω_{NP}
  - Non-perturbative effects are significant!
  - Factorization validity improves to higher z_{cut}

$$\frac{d\sigma_{\text{had.}}}{dx\,dQ^2\,dm^2_{\text{gr.}}} = \int d\epsilon\,\frac{d\sigma}{dx\,dQ^2\,dm^2_{\text{gr.}}}\left(m^2_{\text{gr.}} - \frac{\epsilon^2}{z_{\text{cut}}}\right) f_{\text{mod.}}(\epsilon)\,,$$

$$f_{\text{mod.}}(\epsilon) = N_{\text{mod.}}\,\frac{4\epsilon}{\Omega^2}\,\exp\left(\frac{2\epsilon}{\Omega}\right)$$

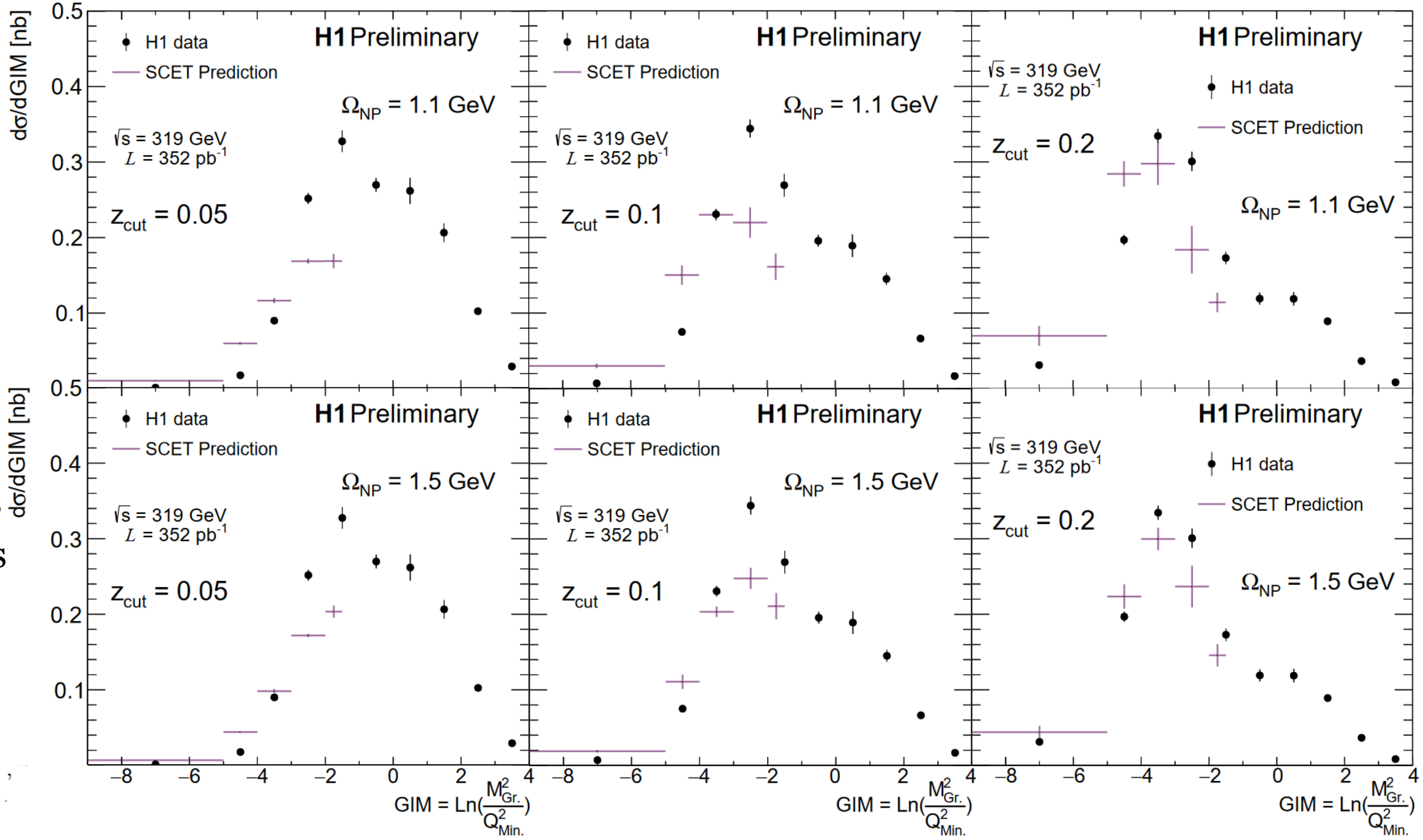

Groomed Invariant Mass - EIC

- At small invariant masses, individual hadron masses play a large role
- Analytic prediction formulated at small masses, in the region defined by:

$$1 \gg z_{\text{cut}} \gg m_{\text{gr.}}^2/Q^2$$

- EIC will have advantages in this region
  - Hadron ID, high statistics
- More differential measurement possible
- New theory tools+data for high-precision studies of NP sector
- Small angles also important
  - Good angular resolution needed

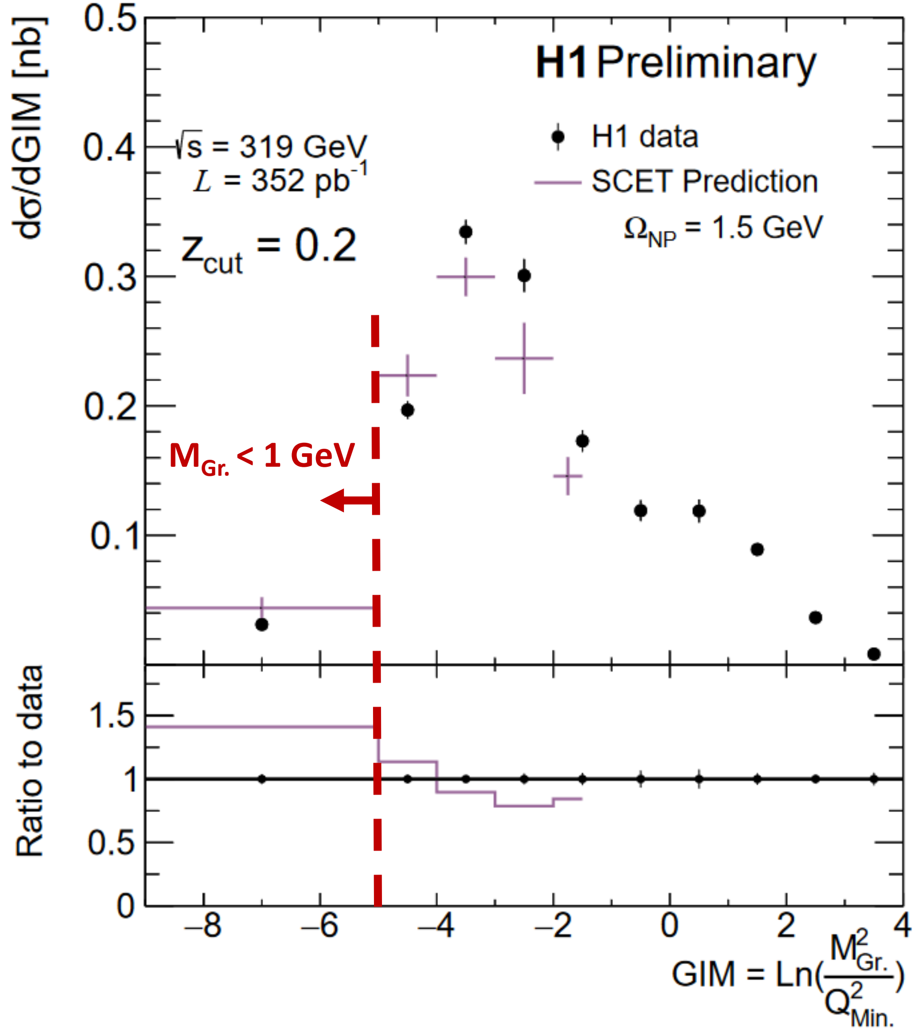

Lessons for EIC – Breit Frame

- **Good reconstruction of event kinematics is vital for performing measurements in the Breit frame**

- Breit frame is a powerful tool for jet-related studies, but comes with additional uncertainty from boost reconstruction that needs to be under control

- QED ISR/FSR can have devastating effects on Breit frame measurements if not properly handled
  - These photons are typically quite energetic and at midrapidity in the Breit frame
  - Easy to confuse for interesting hadronic final state effects!

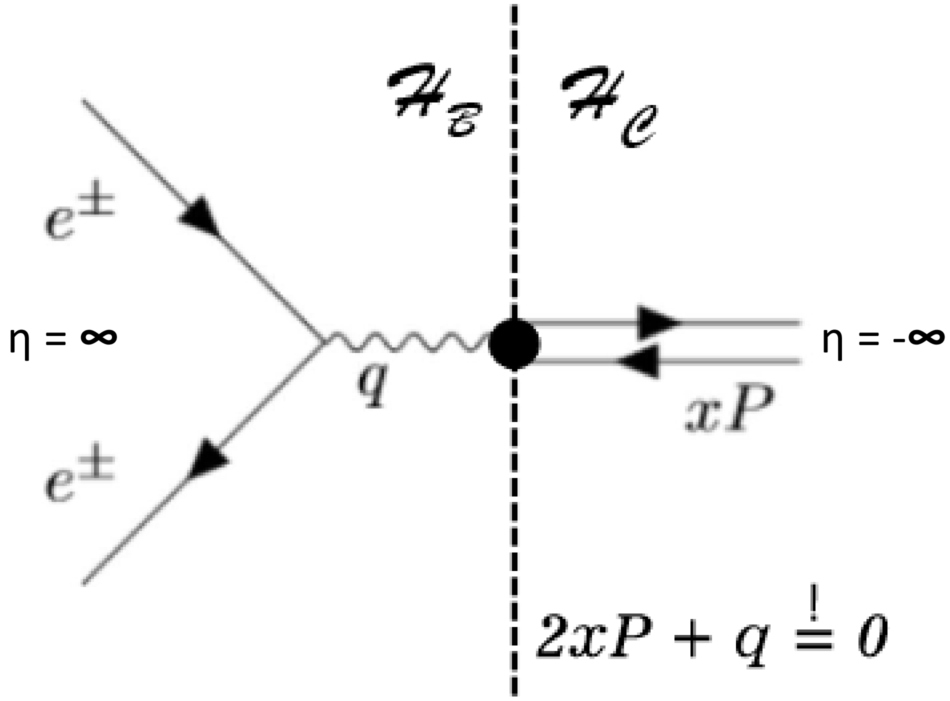

Lessons for EIC – E - P_z

$$\Sigma = \sum_h (E_h - p_{z,h})$$

- IΣ method first described by Bernardi & Bassler in 1994
  - hep-ex/9412004
- For this analysis, the IΣ method yielded the best boost reconstruction and thus the highest purity for the measurement
- This method clearly relies very heavily on the measurement of Σ

$$\Sigma = \sum_h (E_h - p_{z,h})$$

- E-P_z maximized by particles in electron-going (-z) direction, large for barrel, small for forward-going
  - Important to reconstruct backward + barrel momenta well
  - At low-x, IΣ method is similar to electron method in resolution, hadrons go mostly backward

$$E_{I\Sigma}^{e'} = \frac{\Sigma_{HFS} + E_{e'}(1 - \cos\theta_{e'})}{2}$$

$$x_{I\Sigma} = \frac{E_{e'}}{E_p} \frac{\cos^2\theta/2}{y_\Sigma}$$

$$y_{I\Sigma} = y_\Sigma = \frac{\Sigma}{\Sigma + E(1 - \cos\theta)}$$

$$Q^2_{I\Sigma} = \frac{E^2 \sin^2\theta}{1 - y_\Sigma}$$

Conclusion

- H1 has performed the first measurement of groomed event shapes in DIS
  - H1prelim-22-033
  - See also the ungroomed 1-jettiness preliminary: H1prelim-21-032
- Data has been compared to a variety of MC predictions from SHERPA*, PYTHIA, HERWIG, DJANGOH, RAPGAP, as well as analytic predictions from SCET
  - Signifies that DIS MC models could use improvement, especially with EIC fast approaching
    - HERA data will necessarily play an important role in this initiative!
- Good Breit frame reconstruction enables a wide range of QCD studies
  - Jets, TMDs, spin, hadronic physics, things yet unstudied → maximize capability for generic tools

***SHERPA authors already undertaking a DIS tuning campaign utilizing this data!**

Bibliography

[1] - Revisiting the role of grooming in DIS, Y. Makris - arXiv:2101.02708

[2] – Groomed and energy-energy-correlation event shapes at EIC, Y. Makris - LBL Seminar: Oct. 2020

[3] – PYTHIA 8.3 Manual - arXiv:2203.11601

[4] – SHERPA 2.2.12 Manual - sherpa.hepforge.org/doc/SHERPA-MC-2.2.12.html

[5] – herwig.hepforge.org

Backup

H1 Detector

- HERA
  - World's only high energy electron-proton collider

$$E_e = 27.6\ \text{GeV}, E_p = 920\ \text{GeV}$$
$$\rightarrow \sqrt{s} = 319\ \text{GeV}$$

  - 352 pb^{-1} collected in HERA-II run period from 2003-2007
- H1 Experiment
  - Hermetic detector with asymmetric design
    - Drift chamber + silicon tracking
    - High-resolution LAr calorimeter
  - Trigger on high-energy hadronic or EM LAr cluster
    - > 99% efficient for $y < 0.7$

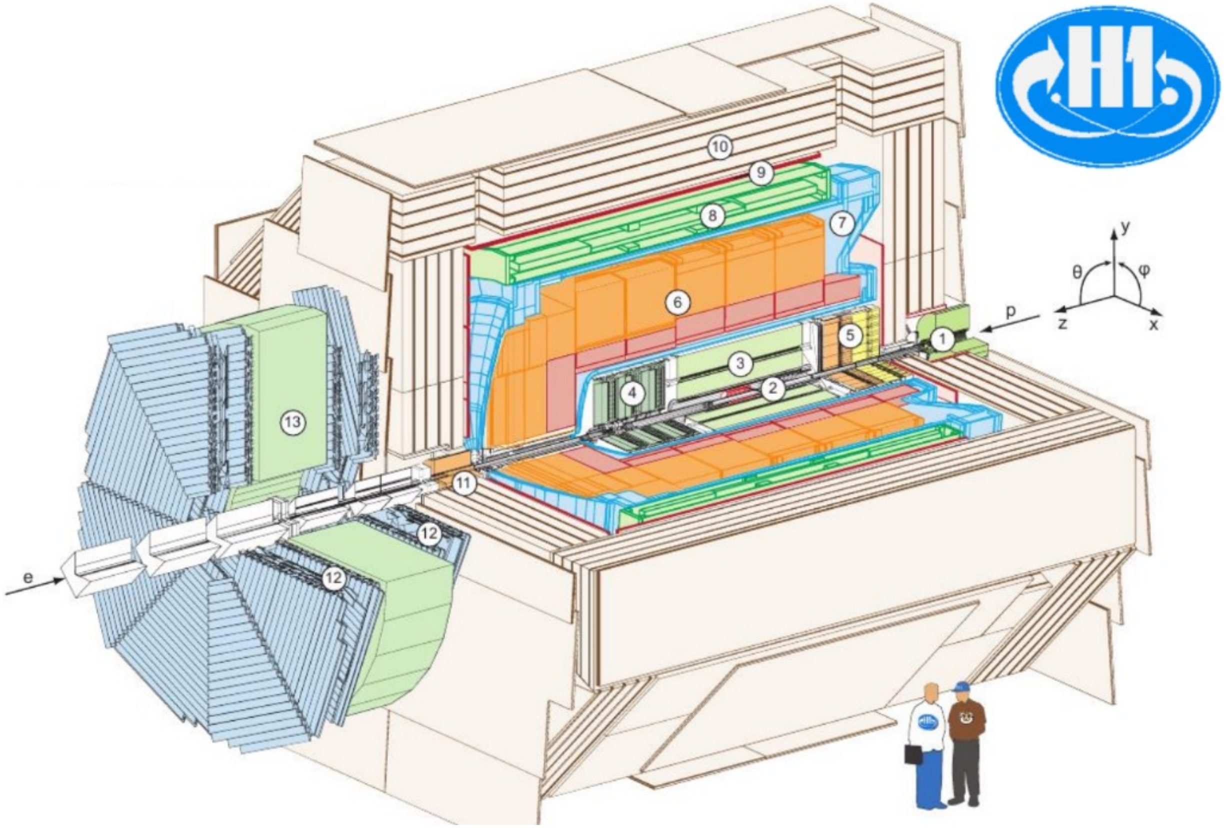

H1 LAr Calorimeter Specifications

Electromagnetic part	Hadronic part
10 to 100 cm^2	50 to 2000 cm^2
20 to 30 X_0 (30784)	4.7 to 7 λ_{abs} (13568)
$\approx 11\%/\sqrt{E_e} \oplus 1\%$	$\approx 50\%/\sqrt{E_h} \oplus 2\%$

Lessons for EIC - QED

- ISR typically unmeasured in detector
  - For observables where all final state particles contribute, radiative MC can give significantly different results if ISR photon is included in final state
  - $E-P_z$ cut helps
  - Having radiative and non-radiative MC
- Typically want to compare data (radiative) to QCD theory (non-radiative)
  - If you don't measure the photon, only have to correct for lower e_{beam} energy at hard vertex

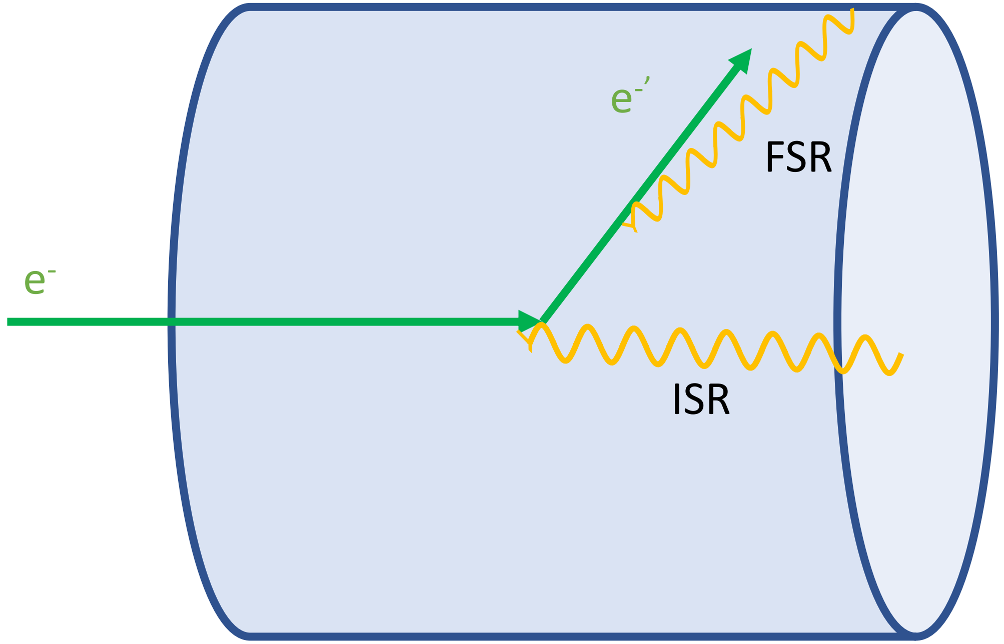

Lessons for EIC - QED

- FSR handled by recombining particles within a lab-frame cone of R = 0.2 of the scattered electron with the scattered election
  - FSR photon is very close to scattered election, typically within calorimeter position resolution
  - FSR photon conversions can fake as HFS tracks

- Cone cut removes genuine HFS particle only 0.75% of the time, typically low energy
  - Momentum balance disfavors HFS particles being near election

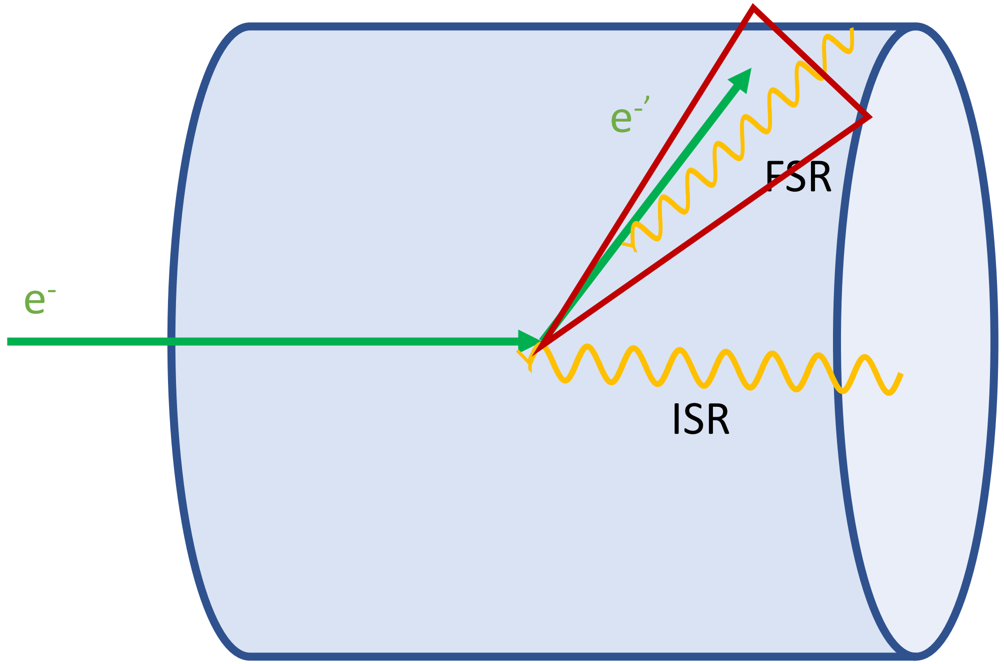

Lessons for EIC – Kine Reco

- At HERA, electron method was made difficult in kinematic regions where the electron was low energy (high y) and/or near to HFS particles (low x)
  - These regions are vital to EIC physics
- At EIC, PID detectors should make purity of scattered electron a bit better
  - Low mass detectors will also improve the feasibility of the electron method
- However, electron method will always suffer from QED radiation

$$\Sigma = \sum_h (E_h - p_{z,h})$$

$$E_{I\Sigma}^{e'} = \frac{\Sigma_{HFS} + E_{e'}(1 - \cos\theta_{e'})}{2}$$

$$x_{I\Sigma} = \frac{E_{e'}}{E_p} \frac{\cos^2\theta/2}{y_\Sigma}$$

$$y_{I\Sigma} = y_\Sigma = \frac{\Sigma}{\Sigma + E(1 - \cos\theta)}$$

$$Q^2_{I\Sigma} = \frac{E^2 \sin^2\theta}{1 - y_\Sigma}$$

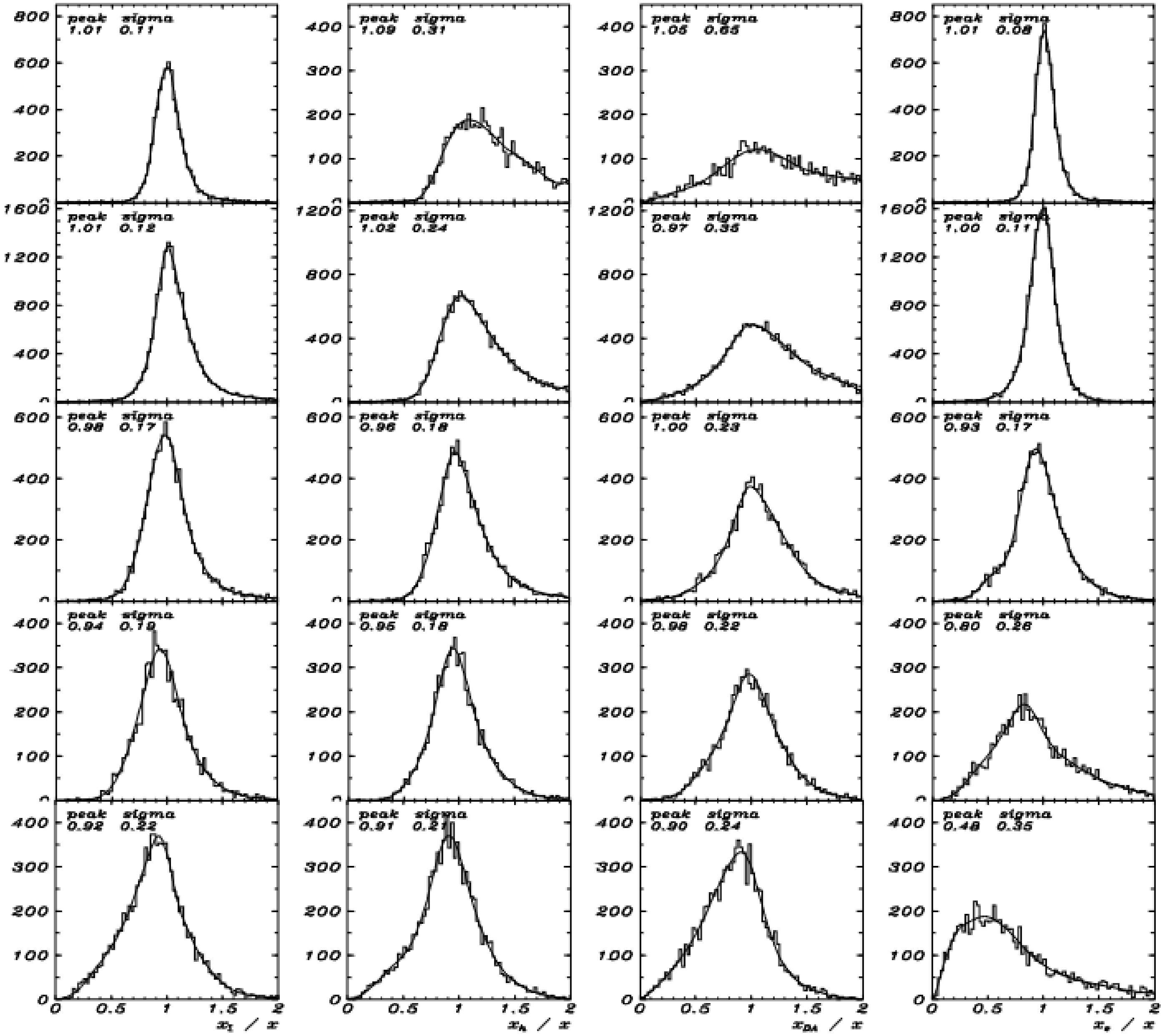

Figure 2: Comparison x_{method}/x at low Q^2 ($Q^2 > 7$ GeV^2) for the Σ, mixed , DA and e methods. From top to bottom, each row represent a bin in y: very high (0.5-0.8), high (0.2-0.5), medium (0.1-0.2), low (0.05-0.1), very low (0.01-0.05).

Results

- Data is corrected for real QED ISR and FSR
- Uncertainty on data is statistical ⊕ systematic
- RAPGAP and DJANGOH
  - Standard H1 MCs
  - Both use LEPTO for matrix elements $O(\alpha_S)$
- DJANGOH:
  - Color dipole model for parton shower + string fragmentation
- RAPGAP:
  - DGLAP parton shower + string fragmentation

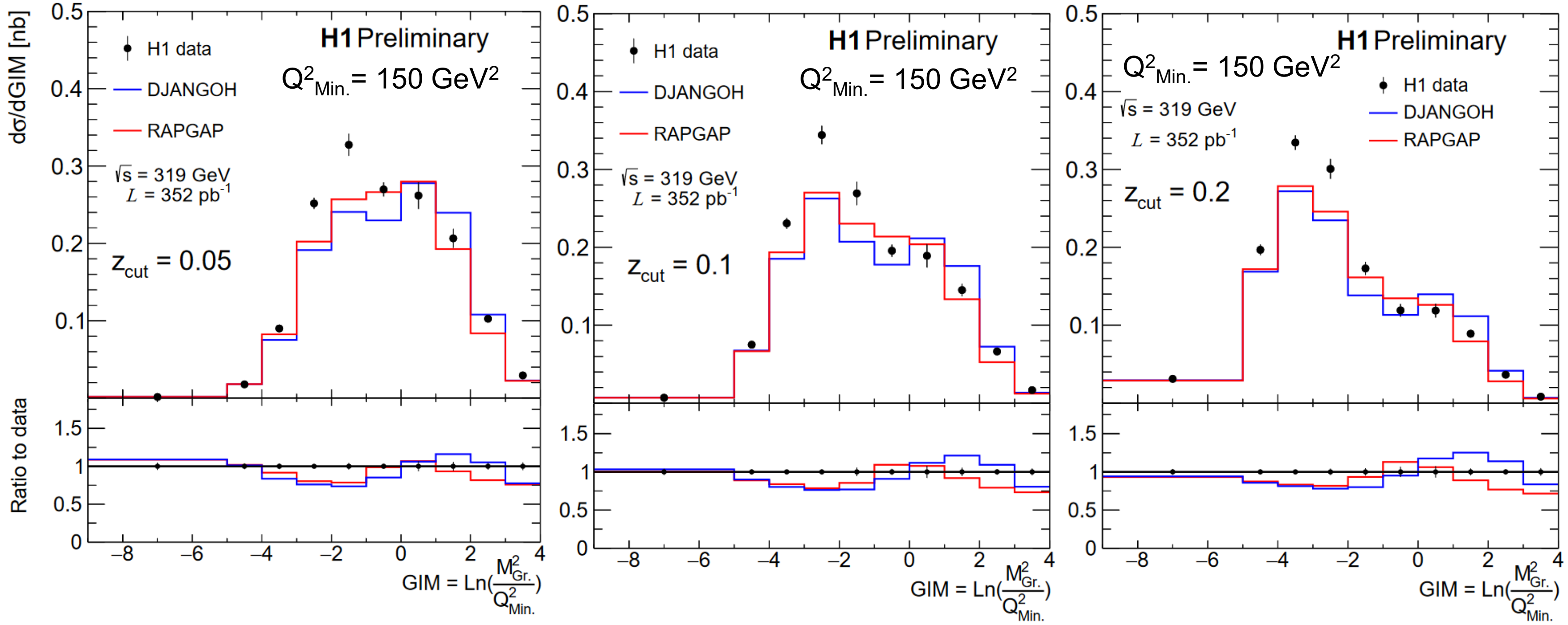

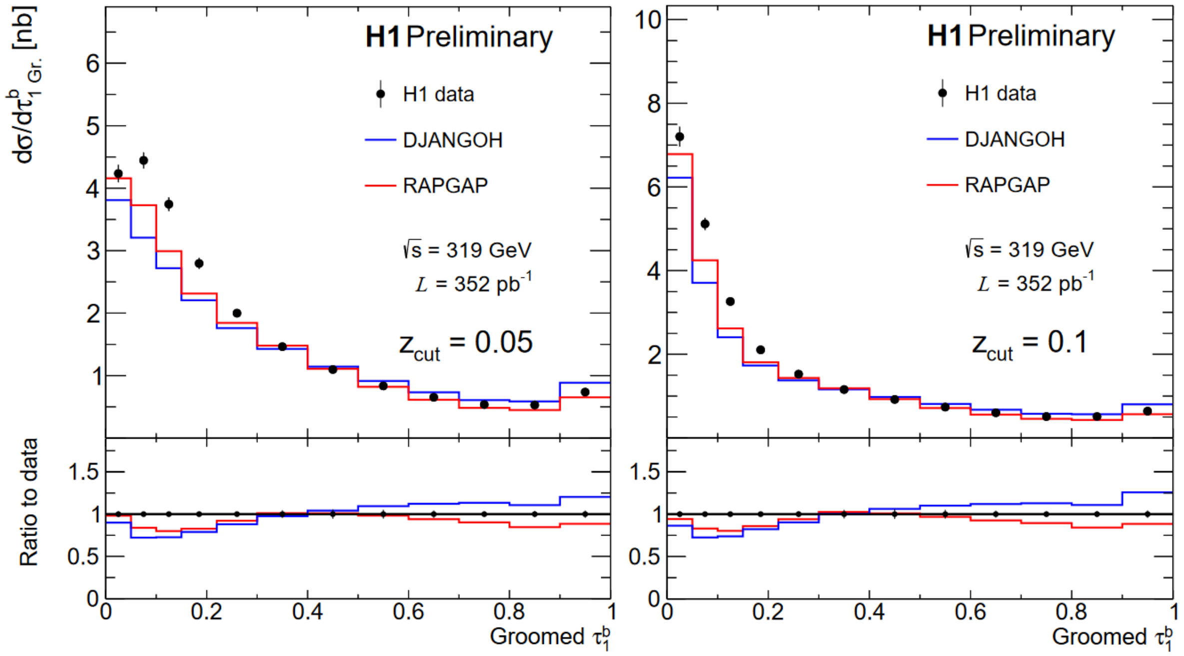

Data is corrected for real QED ISR and FSR
Uncertainty on data is statistical ⊕ systematic
RAPGAP and DJANGOH
- Standard H1 MCs
- Both use LEPTO for matrix elements $O(\alpha_S)$
DJANGOH:
- Color dipole model for parton shower + string fragmentation
RAPGAP:
- DGLAP parton shower + string fragmentation

Results

- SHERPA
  - Version 2.2.12
  - MEPS@NLO
- AHADIC++:
  - SHERPA native cluster hadronization model
- Lund:
  - Lund string model from PYTHIA
- Both models provide good description of fixed-order region

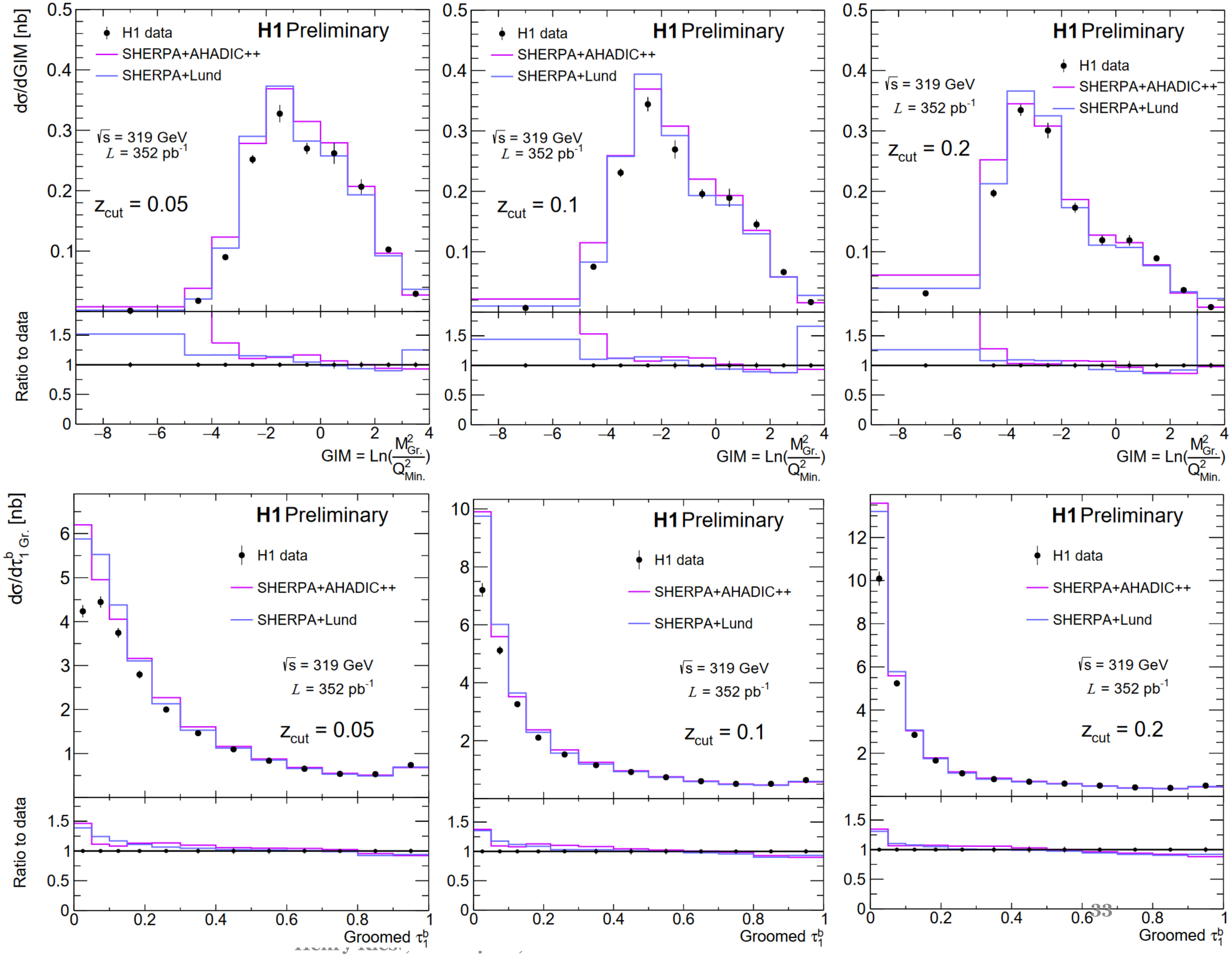

Results

- Herwig
  - Version 7.2.2
- NLO⊕PS:
  - Herwig internal implementation of MC@NLO via Matchbox
- Merging:
  - Dipole shower with multijet merging

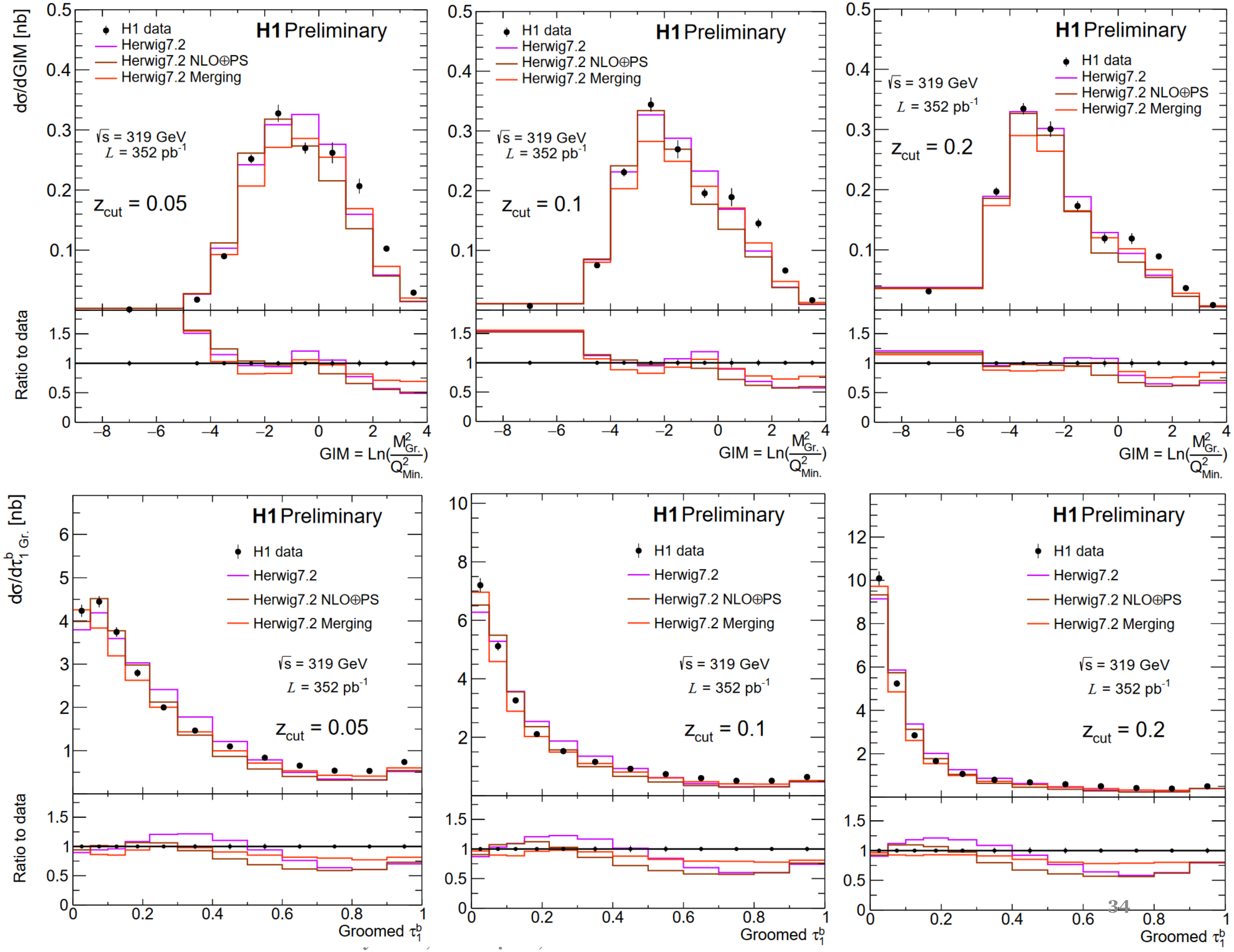

Results

- PYTHIA
  - Version 8.3
  - No external matrix elements
- DIRE:
  - Dipole resummation
  - Excellent description in resummation region
- VINCIA:
  - Antenna shower

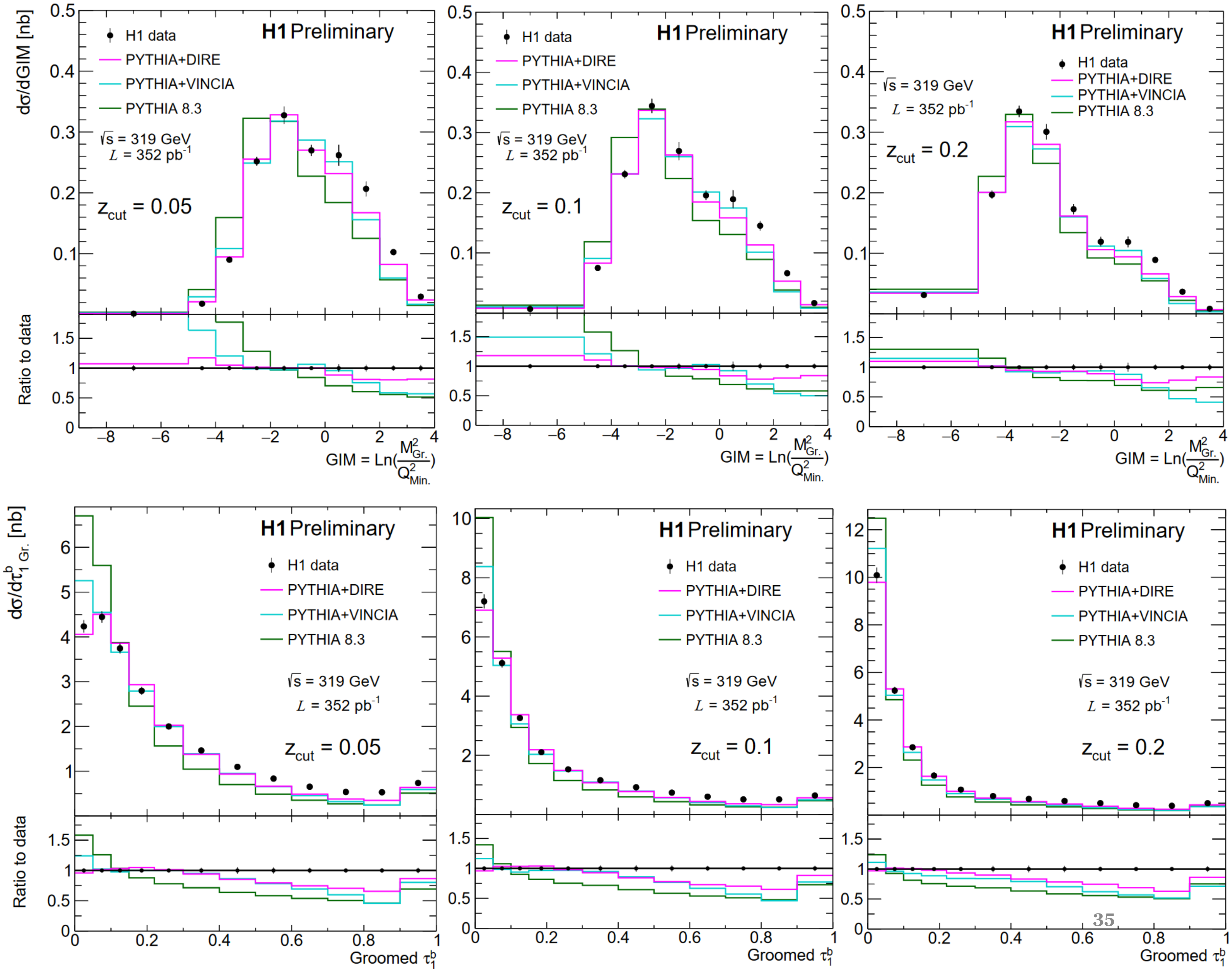

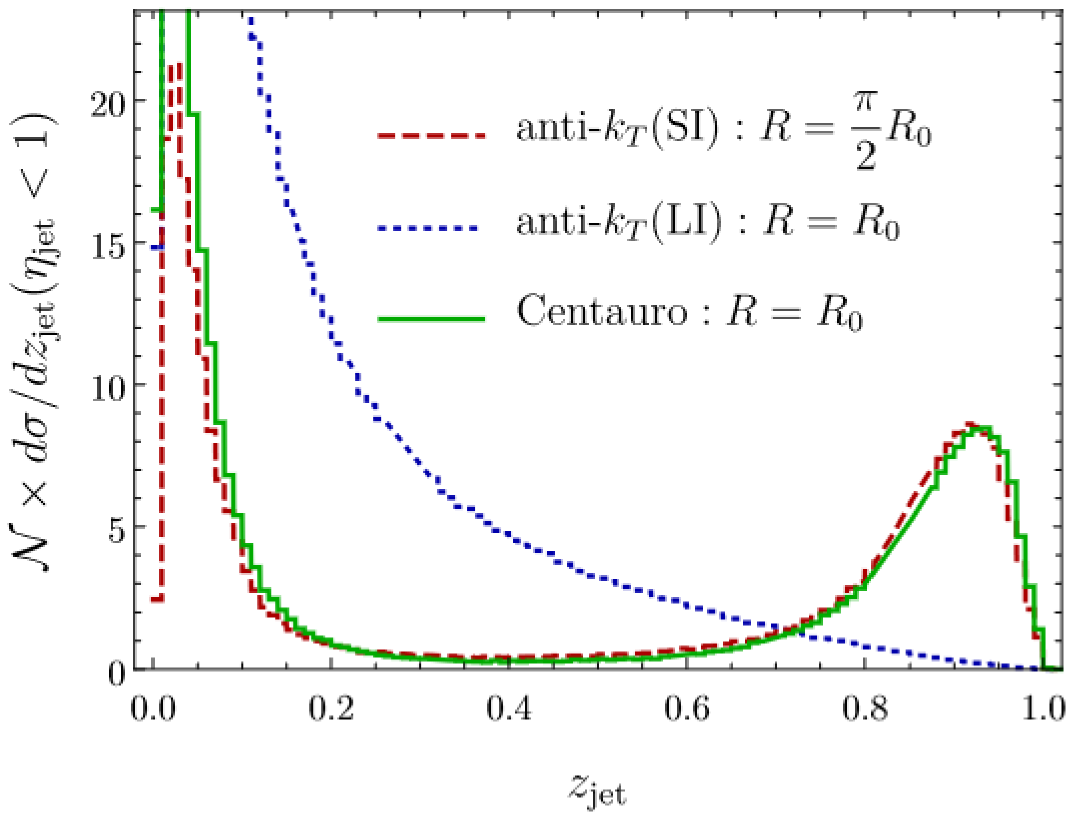

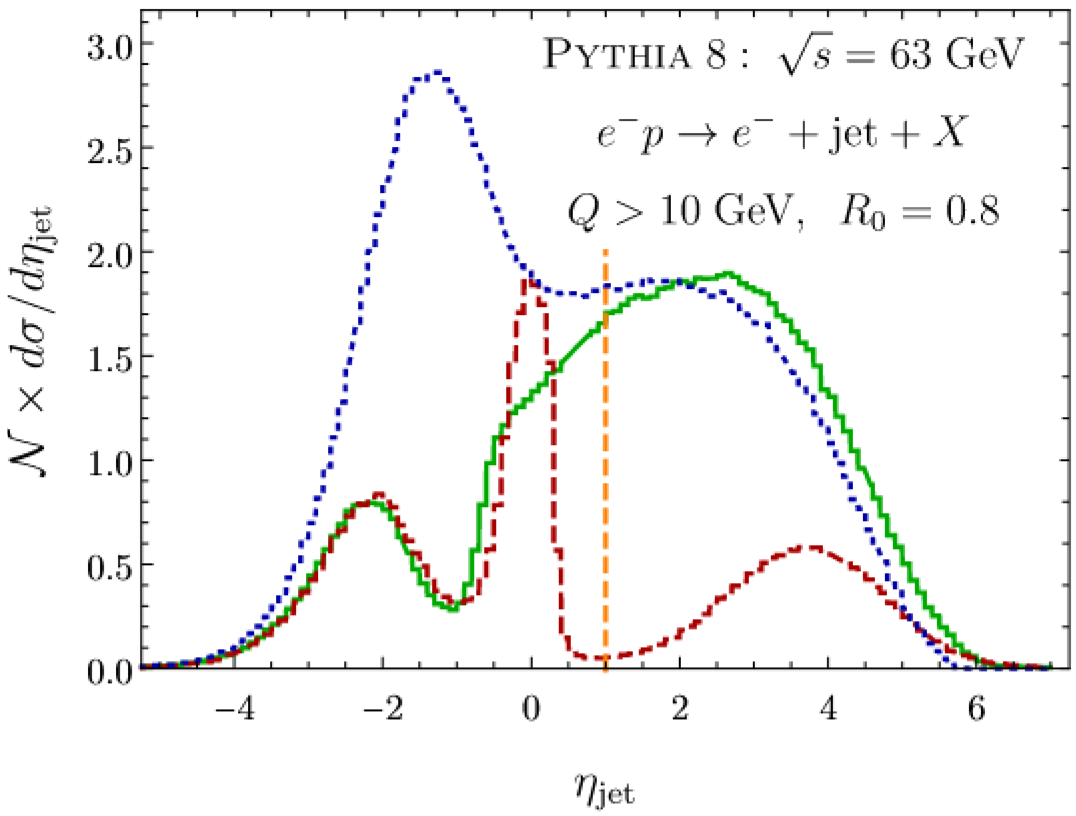

Figure 4. Pseudorapidity (top panel) and momentum fraction $z_{\rm jet}$ (bottom panel) of jets clustered with anti-k_T(LI), anti-k_T(LI) and Centauro algorithms in the Breit frame. Here $\mathcal{N}$ is an overall normalization constant chosen to improve readability and is the same for all curves in a graph.

Stony Brook University

Centauro

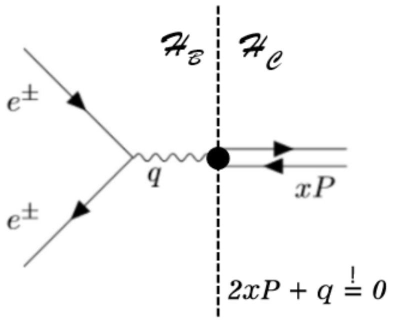

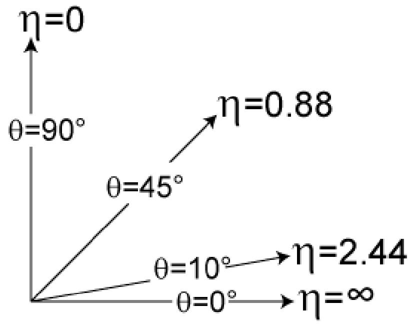

- Jet algorithm with asymmetric clustering measure
  - Treat current hemisphere and beam hemisphere differently
- Typical longitudinally-invariant jet algorithms cluster in (rapidity, azimuthal angle) space and fail to capture the born-level configuration in the Breit frame
  - Particles close to struck-parton direction have divergent rapidity, and therefore divergent distance between each other!
    - Makes study of single-jet Born level configuration impossible!
- Use spherically invariant clustering (polar angle, azimuthal angle) in the struck-parton direction and longitudinally invariant in beam direction
- Tends to create one hard jet in struck-parton direction and many weak single particle jets in beam direction, which can easily be filtered away

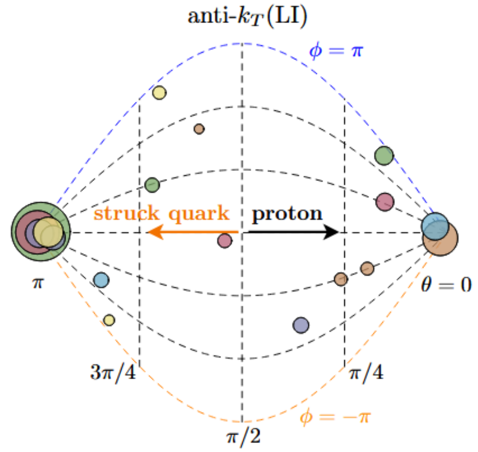

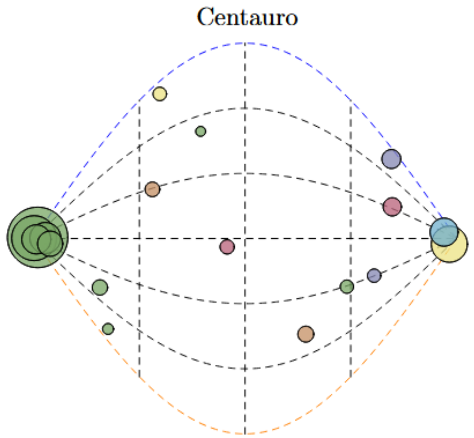

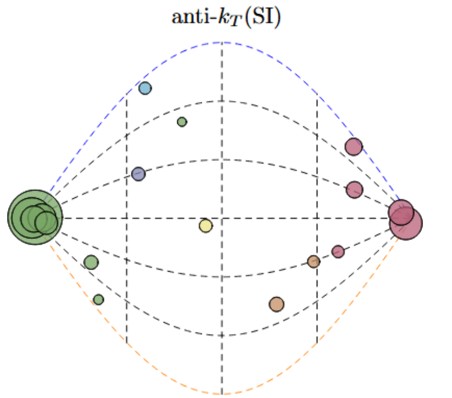

Stony Brook University

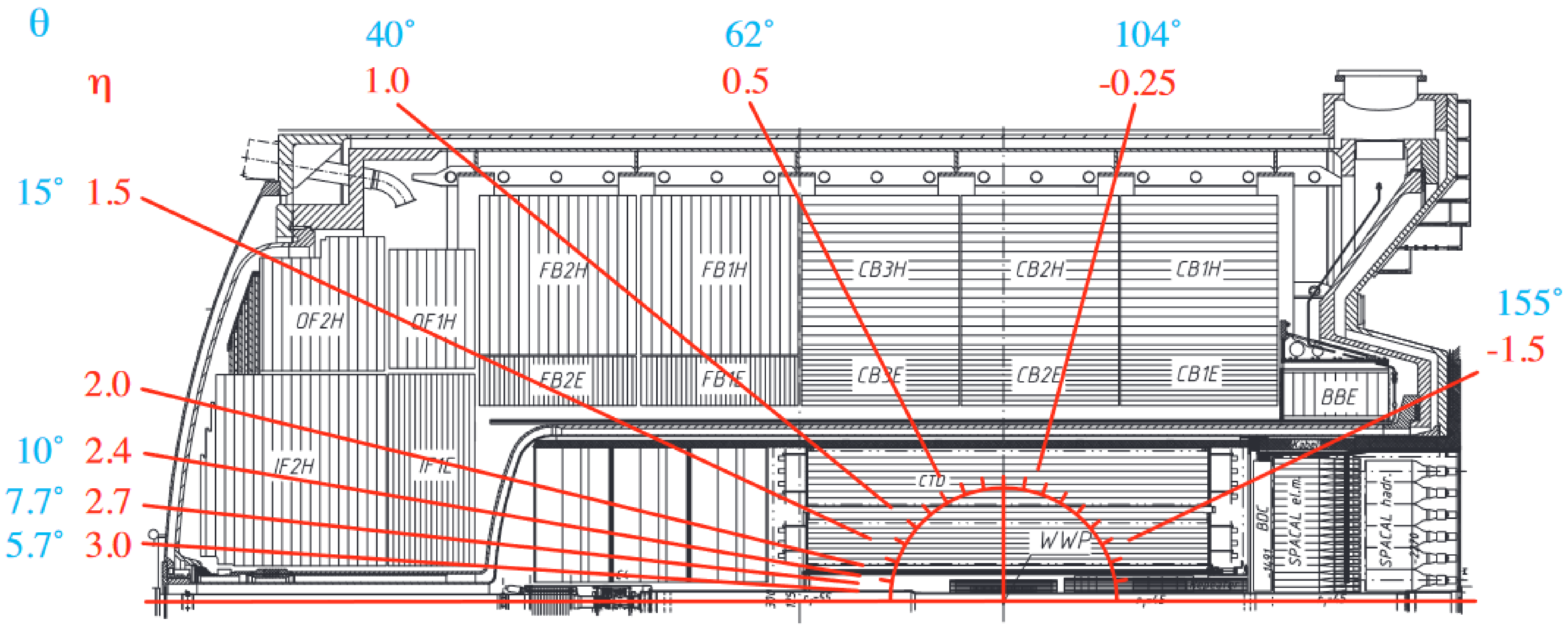

Figure 8.9: Pseudorapidity regions in the H1 detector.

FAR BEYOND

z_{cut}	0.05	0.1	0.2
Pythia8.3	0.31%	1.3%	6.3%
Pythia+Vincia	0.52%	1.7%	6.9%
Pythia+DIRE	0.47%	1.2%	5.6%
SHERPA+AHADIC++	0.03%	0.31%	3.6%
SHERPA+LUND	0.09%	0.59%	4.9%
HERWIG	0.038%	0.36%	3.6%
HERWIG+Merging	0.04%	0.39%	3.6%
HERWIG+MC@NLO	0.04%	0.39%	3.8%
DJANGO (Gen.)	0.09%	0.5%	4.0%
RAPGAP (Gen.)	0.07%	0.4%	3.7%
DJANGO (Det.)	1.0%	2.3%	7.8%
RAPGAP (Det.)	0.9%	2.2%	7.6%

Table 1: Percentage of events that fail grooming. Rapgap and Djangoh are listed for both detector and generator level.